## Plant Physiology®

# Heritable changes of epialleles near genes in maize can be triggered in the absence of CHH methylation

Beibei Liu, Diya Yang, Dafang Wang, Chun Liang, Jianping Wang, Damon Lisch, and Meixia Zhao, S.\*

- 1 Department of Biology, Miami University, Oxford, OH 45056, USA
- 2 Biology Department, Hofstra University, Hempstead, NY 11549, USA
- 3 Agronomy Department, University of Florida, Gainesville, FL 32610, USA
- 4 Department of Botany and Plant Pathology, Purdue University, West Lafayette, IN 47907, USA
- 5 Department of Microbiology and Cell Science, University of Florida, Gainesville, FL 32611, USA

The author responsible for distribution of materials integral to the findings presented in this article in accordance with the policy described in the Instructions for Authors (https://academic.oup.com/plphys/pages/General-Instructions) is: Meixia Zhao (meixiazhao@ufl.edu).

#### **Abstract**

Research Article

Trans-chromosomal interactions resulting in changes in DNA methylation during hybridization have been observed in several plant species. However, little is known about the causes or consequences of these interactions. Here, we compared DNA methylomes of F1 hybrids that are mutant for a small RNA biogenesis gene, Mop1 (Mediator of paramutation1), with that of their parents, wild-type siblings, and backcrossed progeny in maize (Zea mays). Our data show that hybridization triggers global changes in both trans-chromosomal methylation (TCM) and trans-chromosomal demethylation (TCdM), most of which involved changes in CHH methylation. In more than 60% of these TCM differentially methylated regions (DMRs) in which small RNAs are available, no significant changes in the quantity of small RNAs were observed. Methylation at the CHH TCM DMRs was largely lost in the mop1 mutant, although the effects of this mutant varied depending on the location of these DMRs. Interestingly, an increase in CHH at TCM DMRs was associated with enhanced expression of a subset of highly expressed genes and suppressed expression of a small number of lowly expressed genes. Examination of the methylation levels in backcrossed plants demonstrates that both TCM and TCdM can be maintained in the subsequent generation, but that TCdM is more stable than TCM. Surprisingly, although increased CHH methylation in most TCM DMRs in F1 plants required Mop1, initiation of a new epigenetic state of these DMRs did not require a functional copy of this gene, suggesting that initiation of these changes is independent of RNA-directed DNA methylation.

#### Introduction

DNA methylation is a heritable epigenetic mark involved in many important biological processes, such as genome stability, genomic imprinting, paramutation, development, and environmental stress responses (Matzke et al. 2015; Lewsey et al. 2016; Zhang et al. 2016; Erdmann and Picard 2020). In plants, DNA methylation commonly occurs in 3 cytosine contexts, the symmetric CG and CHG (where H = A, C, or T) contexts

and the asymmetric CHH context (Law and Jacobsen 2010; Matzke and Mosher 2014; Li et al. 2015a). In Arabidopsis (Arabidopsis thaliana), de novo methylation at all these 3 cytosine contexts is catalyzed by DOMAINS REARRANGED METHYLTRANSFERASE 2 (DRM2) through the RNA-directed DNA methylation (RdDM) pathway. In RdDM, single-stranded RNA is transcribed by RNA polymerase IV (Pol IV) and copied into double-stranded RNA by RNA DEPENDENT RNA

**Open Access** 

<sup>\*</sup>Author for correspondence: meixiazhao@ufl.edu

POLYMERASE 2 (RDR2). The dsRNA is then processed by DICER-LIKE 3 (DCL3) into 24-nucleotide (nt) small interfering RNAs (siRNAs), which can recruit histone modifiers and DNA methyltransferases back to the original DNA sequences to trigger methylation (Matzke and Mosher 2014; Matzke et al. 2015; Erdmann and Picard 2020). In maize (Zea mays), loci targeted by RdDM are primarily transposable elements (TEs) or other repeats near genes, where the chromatin is more accessible, rather than the deeply heterochromatic regions farther from genes (Gent et al. 2014; Li et al. 2015a). In plants, DNA methylation is maintained by different pathways depending on the location of the target sequences (Law and Jacobsen 2010). CG and CHG methylation are maintained during DNA replication by METHYTRANSFERASE 1 (MET1) and CHROMOMETHYLASE 3 (CMT3), respectively (Matzke and Mosher 2014; Matzke et al. 2015). CHH methylation is maintained through persistent de novo methylation by DRM2 through the RdDM pathway, which requires small RNAs and relatively open chromatin, or by CHROMOMETHYLASE 2 (CMT2) in conjunction with histone H3 lysine 9 dimethylation (H3K9me2) in deep heterochromatin, which does not (Stroud et al. 2014).

This complex system of chromatin modification ensures that epigenetic silencing is reliably transmitted from generation to generation. However, there are situations in which that stability can be perturbed. Hybrids are an example of this because hybridization brings together 2 divergent genomes and epigenomes in the same nucleus. The interaction between these divergent genomes can result in both instability and transfers of epigenetic information between genomes. Trans-chromosomal interactions of DNA methylation between parental alleles in F1 hybrids occur in many plant species, including Arabidopsis (Greaves et al. 2012; Shen et al. 2012; Greaves et al. 2015, 2016; Zhang et al. 2016), rice (Oryza sativa; He et al. 2010; Chodavarapu et al. 2012; Ma et al. 2021), maize (Barber et al. 2012; He et al. 2013; Li et al. 2014a), pigeonpea (Cajanus cajan; Junaid et al. 2018), and soybean (Glycine max; Schmitz et al. 2013). In Arabidopsis F1 hybrids, substantial changes in F1 methylomes involve trans-chromosomal methylation (TCM) and trans-chromosomal demethylation (TCdM), in which the methylation level of 1 parental allele is altered to resemble that of the other parental allele (Greaves et al. 2012, 2016; Zhang et al. 2016; Junaid et al. 2018).

Small RNAs, particularly 24-nt siRNAs, are associated with the methylation changes at the regions of the genome where methylation levels differ between the 2 parents (He et al. 2010; Groszmann et al. 2011; Chodavarapu et al. 2012; Shivaprasad et al. 2012; Greaves et al. 2016; Zhang et al. 2016). Small RNA sequencing in Arabidopsis, maize, wheat (Aegilops tauschii and Triticum turgidum), and rice has revealed a general decrease in 24-nt siRNAs in hybrids at regions where parental siRNA abundance differs (He et al. 2010; Groszmann et al. 2011; Kenan-Eichler et al. 2011; Barber et al. 2012; Chodavarapu et al. 2012). In maize, downregulation of 24-nt siRNAs following hybridization is

observed in developing ears but not in seedling shoot apex (Barber et al. 2012), suggesting either the tissue type or developmental stage is important for the changes in small RNAs observed in hybrids. It has been hypothesized that siRNAs produced from the methylated parental allele can trigger de novo methylation of the other parental allele when the 2 alleles are brought together in F1 hybrids (Greaves et al. 2012, 2015), a process that is reminiscent of paramutation at many loci in maize (Arteaga-Vazquez and Chandler 2010; Hollick 2017). In Arabidopsis F1 hybrids, siRNAs from 1 allele are found to be sufficient to trigger methylation without triggering siRNA biogenesis from the other allele in F1 plants at TCM differentially methylated regions (DMRs; Zhang et al. 2016).

The inheritance of both TCM and TCdM in subsequent generations can be meiotically stable across many generations but varies at different loci in Arabidopsis (Schmitz et al. 2011; Greaves et al. 2014, 2016). In maize and soybean, parental methylation differences are inherited by recombinant inbred lines over multiple generations. However, these changes can be unstable and are likely guided by small RNAs (Regulski et al. 2013; Schmitz et al. 2013). A recent study in maize identified thousands of TCM and TCdM loci in F1 hybrids. However, only about 3% of these changes were transmitted through 6 generations of backcrossing and 3 generations of selfing (Cao et al. 2022), suggesting that the methylation status of any given locus is largely determined by local sequences.

Most recent research has focused on the initiation and maintenance of overall levels of DNA methylation, but the causes and consequences of DNA methylation depend on its sequence context (Li et al. 2015b). In large genomes such as maize, regions distant from genes are typically maintained in a deeply heterochromatic state, and cytosine methylation is primarily the CG and CHG sequence contexts. In contrast, CHH methylation, which is primarily dependent on RdDM in maize, occurs almost exclusively in regions immediately adjacent to genes, resulting in the so-called "mCHH islands" (Gent et al. 2013; Li et al. 2015a). The result of this variation is a dramatically skewed distribution of methylated cytosines. In the maize reference genome, there are a total of 972,798,068 cytosines, out of which 18.7% and 16.4% are CG and CHG cytosines and 64.9% of which are CHH cytosines. Unlike CG and CHG cytosines, which are methylated at a high level, the level of CHH methylation is extremely low, only 2.4% genome-wide, and is largely restricted to mCHH islands. This may be due to lack of CMT2 in maize, the major chromomethylase that functions in the maintenance of CHH methylation in heterochromatin in other plants. In maize, these CHH islands are thought to be the boundaries between deeply silenced heterochromatin and more active euchromatin that promote and reinforce silencing of TEs near genes (Gent et al. 2013; Li et al. 2015a).

To address these questions, we performed highthroughput sequencing of DNA methylomes, small RNA, and mRNA from F1 hybrids that were mutant for a small RNA biogenesis gene, Mop1 (Mediator of paramutation1), as well as their parents, wild-type siblings, and backcrossed (BC1) progeny. Mop1 is a putative ortholog of RDR2 in Arabidopsis, which is a major component of the RdDM pathway (Alleman et al. 2006; Woodhouse et al. 2006). In the mop1 mutant, 24-nt siRNAs are dramatically reduced (Nobuta et al. 2008; Gent et al. 2014), which results in a near complete removal of CHH methylation near genes (Li et al. 2015a; Zhao et al. 2021), confirming a major role for MOP1 in de novo CHH methylation in maize. Our results show a global increase in CHH methylation in hybrids, but these increases are unequally distributed, leading to new and distinctive patterns of methylation. While only the lowparent (the parent with the lower methylation level) allele gained methylation in CG and CHG TCM DMRs, both the high-parent (the parent with the higher methylation level) and low-parent alleles of CHH TCM DMRs gained methylation in F1 hybrids. As has been observed in Arabidopsis, the increase in methylation in the low-parent alleles was not associated with the generation of allele-specific small RNAs at many genomic loci, suggesting that small RNAs from 1 allele are sufficient to trigger methylation in the other allele, but are not always sufficient to trigger Pol IV transcription of the target allele. Interestingly, these CHH TCM DMRs were associated with the enhanced expression of a subset of highly expressed genes and suppressed expression of a subset of lowly expressed genes.

Changes in CG and CHG methylation were often retained in the BC1 generation, a process that did not require MOP1. Heritable changes in CHH methylation were more complex. The increase in CHH methylation in both the highly methylated and lowly methylated alleles was lost in BC1 plants, even at loci where both alleles were present, suggesting that the global increase we observed in the F1 is a function of heterosis, rather than an interaction between each pair of heterozygous epialleles. However, new methylation added to the low methylation allele could be transmitted to the BC1 plants, even in progeny of plants that were mop1 mutant and that lacked MOP1-dependent siRNAs. This suggests that the transfer of the epigenetic state from high CHH alleles to low CHH alleles, as well as the maintenance of this altered state in the gametophyte, does not require MOP1.

#### **Results**

CHH methylation level is increased globally in hybrids To understand the initiation of DNA methylation, we crossed *mop1* heterozygous plants in the Mo17 and B73 backgrounds to each other (Mo17;*mop1-1*/+ × B73;*mop1-1*/+) to generate F1 hybrid *mop1* mutants (Mo17/B73;*mop1-1*/*mop1-1*, designated as *mop1*F1) and their hybrid homozygous wild-type siblings (Mo17/B73;+/+, designated as WTF1; Fig. 1A). We next performed whole genome bisulfite sequencing (WGBS) of

the 2 parental genotypes (Mo17;+/+ and B73;+/+) and the 2 F1 hybrids (WTF1 and mop1F1; Supplementary Table S1). We also included a synthetic F1 hybrid methylome by pooling an equal number of WGBS reads from both Mo17 and B73 parents to serve as a control. The overall methylation levels of B73 (25.1%) and Mo17 (25%) were similar. We observed a substantial increase in overall methylation levels in WTF1 hybrids (30%) compared to the 2 parents (25%), as has been noted previously in both Arabidopsis and (Supplementary Fig. S1 and Table S2; Zhang et al. 2016; Cao et al. 2022). The increased methylation was primarily driven by the increased CHH methylation, while CG and CHG were not dramatically changed (Fig. 1B; Supplementary Figs. S1 and S2). The synthetic F1 had methylation patterns nearly identical to the midparent value (MPV, the average of the 2 parents), suggesting that the increased CHH methylation observed in the authentic F1 hybrids is caused by transchromosomal interaction and/or hybridization (Fig. 1B; Supplementary Figs. S1 and S2). In both parents and WTF1, the overall levels of CHH methylation tend to be higher in chromosomal arms, likely because there are more mCHH islands near genes in the ends of chromosomes (Li et al. 2015a, 2015b). Interestingly, although the mop1 mutation reduces CHH methylation (Gent et al. 2013; Li et al. 2015a; Zhao et al. 2021), the overall level of CHH methylation in mop1F1 was still higher than that of the 2 wild-type parents (Fig. 1B; Supplementary Fig. S2), suggesting that a substantial portion of the increased de novo CHH methylation in F1 hybrid plants does not require canonical RdDM.

Previous research had shown that mop1 mutants primarily affect mCHH islands near active genes (Gent et al. 2014; Li et al. 2015a). Therefore, we plotted DNA methylation levels of CG, CHG, and CHH within gene bodies, 3 kb upstream of transcription start sites (TSSs) and 3 kb downstream of transcription termination sites (TTSs). In genes, we observed similar patterns with respect to the methylation levels of CG and CHG between parents and F1 hybrids. In contrast, the methylation levels of CHH cytosines both upstream and downstream of genes were dramatically increased in WTF1 plants and dramatically reduced in the mop1F1 mutants relative to the 2 parents (Fig. 1C). We next determined CG, CHG, and CHH methylation levels within TE bodies and their flanking regions. The region flanking the distal edge of TEs relative to genes generally had higher levels of CG and CHG methylation than did the region flanking their proximal edge. CHH methylation was increased in WTF1 hybrids across TE bodies and flanking regions relative to the parents, particularly at the 2 edges of TEs. In line with previous observations (Li et al. 2015a), CHH methylation level at the proximal edge and the adjacent flanking regions of TEs in mop1F1 was lower than that in the 2 parents. In contrast, the CHH methylation level at the distal edge of TEs and the adjacent flanking regions in mop1F1 was only marginally reduced relative to WTF1 and was still higher than that in the parents (Fig. 1D). In the body of TEs, the increase in CHH methylation

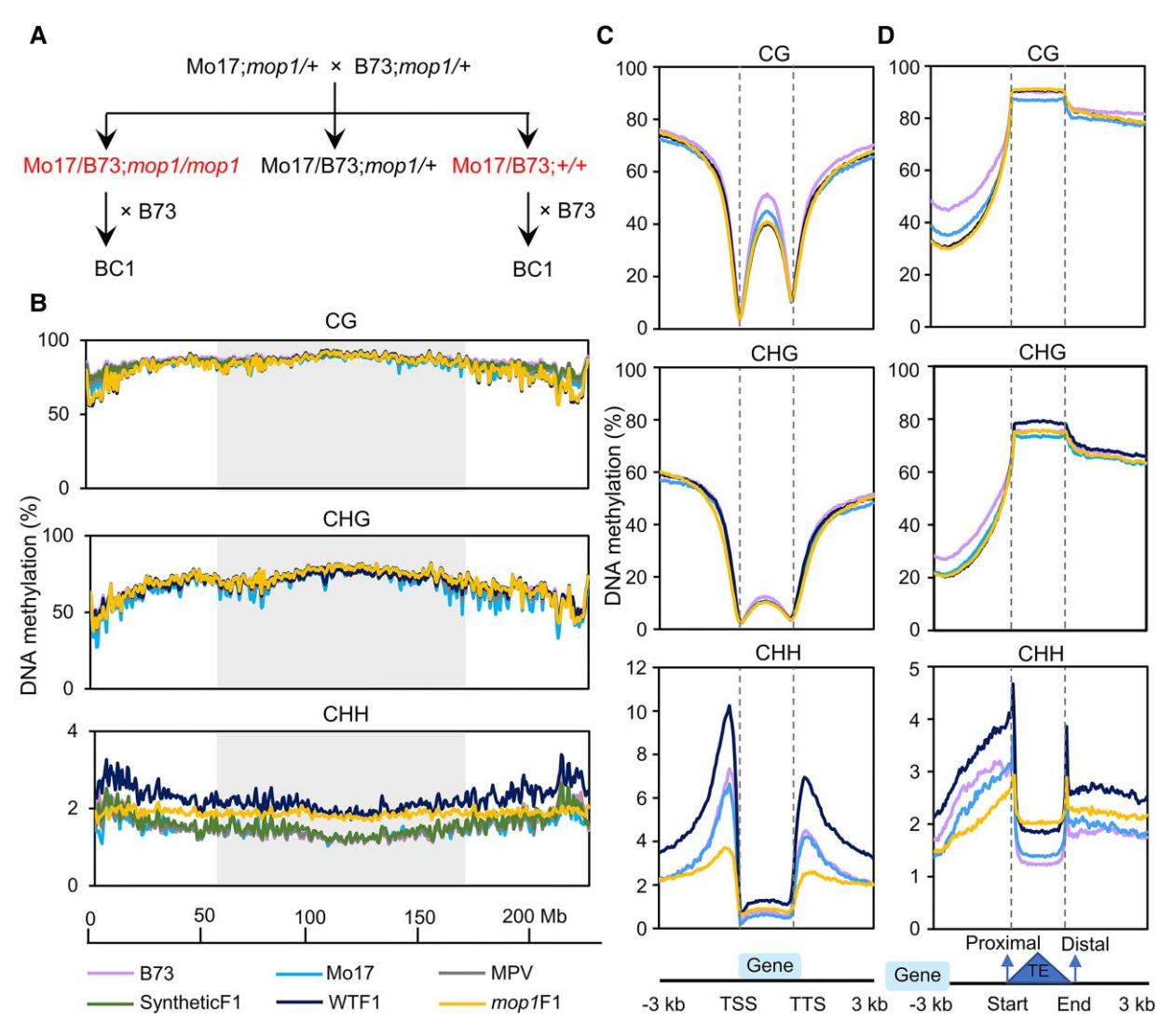


**Figure 1.** CHH methylation level is globally increased in hybrids. **A)** Genetic strategy to construct wild-type F1 (WTF1), *mop1* mutant F1 (*mop1*F1), and BC1. **B)** The distribution of CG, CHG, and CHH methylation on Chromosome 5. Methylation levels were measured in 1 Mb windows with 500 kb shift. The shaded boxes represent pericentromeric regions. MPV, midparent value. The synthetic F1 hybrid methylome was generated by pooling an equal number of WGBS reads from both B73 and Mo17 parents to serve as a control. **C)** Patterns of methylation in and flanking genes. **D)** Patterns of methylation in and flanking TEs. DNA methylation levels were calculated in 50 bp windows in the 3 kb upstream and downstream regions of the genes/TEs. Each gene/TE sequence was divided into 40 equally sized bins to measure the gene/TE body methylation. Bin sizes differ from genes/TEs to genes/TEs because of the different lengths of genes/TEs. The methylation levels of TEs were orientated into proximal and distal ends depending on the flanking genes of TEs. Methylation for each sample was calculated as the proportion of methylated C over total C in each sequence context (CG, CHG, and CHH, where H = A, T, or C) averaged for each window. The average methylation levels were determined by combining 2 biological replicates for each genotype.

triggered by hybridization was unchanged or even increased in *mop1* mutants. Together, these data suggest that MOP1 is particularly important for CHH methylation of the ends of TEs that are near genes, along with the region between the TE and the gene. Outside of those regions, it appears that MOP1 is not required for a substantial portion of the increased CHH methylation in F1 plants. The net effect is a strong effect of *mop1* on CHH islands, but a much-reduced effect on overall changes in DNA methylation seen in the F1 generation.

Levels of CHH methylation of both high- and low-parent (parents with the higher and lower methylation levels) alleles are increased at TCM DMRs in the F1 hybrids

We identified DMRs between the 2 parents, Mo17 and B73, in our data set. We refer to these DMRs as "parental DMRs," which can be Mo17 or B73 hyper-DMRs, indicating that either Mo17 or B73 has a significantly higher level of DNA methylation (Fig. 2A). In total, we identified 7,107 CG, 9,045 CHG, and 13,307 CHH DMRs between the 2 parents

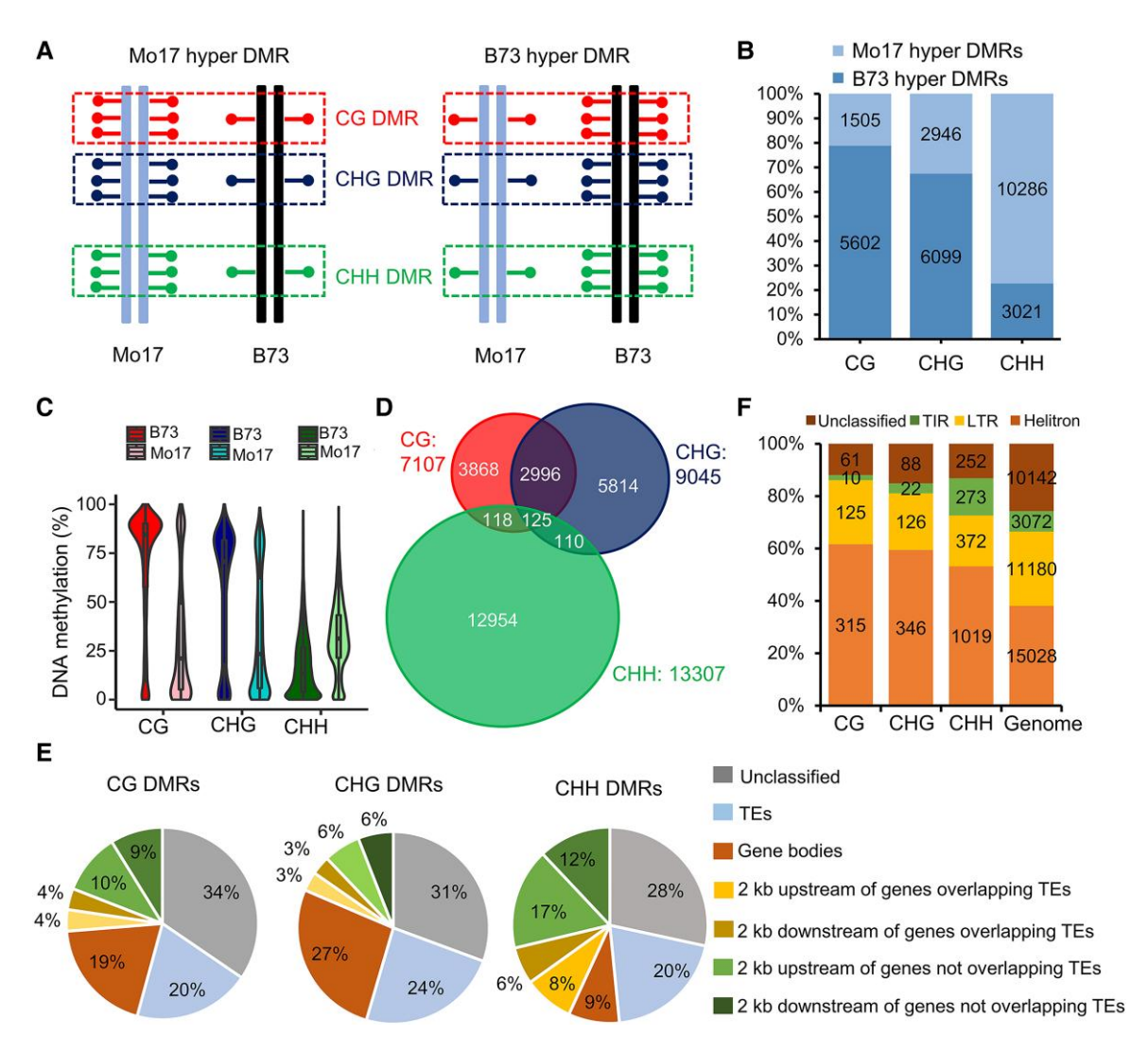


**Figure 2.** Parental CHH DMRs are largely located within 2 kb flanking regions of genes. **A)** Definition of B73 hyper-DMRs (higher methylation in B73) and Mo17 hyper-DMRs (higher methylation in Mo17) between parents. Red (top), blue (middle), and green (bottom) dots represent CG, CHG, and CHH methylation, respectively. **B)** B73 has more CG and CHG hyper-DMRs, and Mo17 has more hyper-CHH DMRs. **C)** B73 has higher methylation levels at CG and CHG DMRs, and Mo17 has higher methylation levels at CHH DMRs. The bottom and top boundaries of the box are the first and third quartiles, and the bold lines within individual boxes are the medians, which are referred to as the second quartiles. The ends of the whiskers (the lines) represent the minimum values and maximum values of the data. **D)** CG and CHG DMRs are more overlapped with each other than each one is with CHH DMRs. **E)** The distribution of CG, CHG, and CHH parental DMRs; 2 kb up- and downstream of genes overlapping TEs indicate that the DMRs overlap TEs within the 2 kb flanking regions of genes. **F)** The types of TEs in the categories of 2 kb up- and downstream of genes overlapping TEs in **E)**. DMRs, differentially methylated regions.

(Fig. 2B; Supplementary Table S3). CHH DMRs, the majority of which ranged from 30 to 90 bp, were generally shorter than CG and CHG DMRs, which typically extended from 200 to 400 bp (Supplementary Fig. S3 and Table S3). The B73 genome had more CG and CHG hyper-DMRs, and the Mo17 genome had more CHH hyper-DMRs, which is consistent with the observation that B73 had higher overall CG and CHG methylation and Mo17 had higher overall CHH methylation at these DMRs (Fig. 2, B and C), as has been noted previously (Li et al. 2014b). To address the concerns with respect to the lower mapping rates of Mo17 reads due to the use of the pseudo-Mo17 genome, we conducted a parallel analysis

using the recently released Mo17 genome sequences as the reference and generated a pseudo-B73 genome (see details in Materials and methods; Chen et al. 2023). We next mapped the WGBS reads from both parents Mo17 and B73 to the authentic Mo17 genome and the pseudo-B73 genome and identified parental DMRs between Mo17 and B73. The data consistently indicated that at these DMRs, B73 exhibited higher levels of CG and CHG methylation, while Mo17 displayed higher levels of CHH methylation (Supplementary Fig. S4).

We also found that CG and CHG DMRs were more overlapped with each other than each one was with CHH

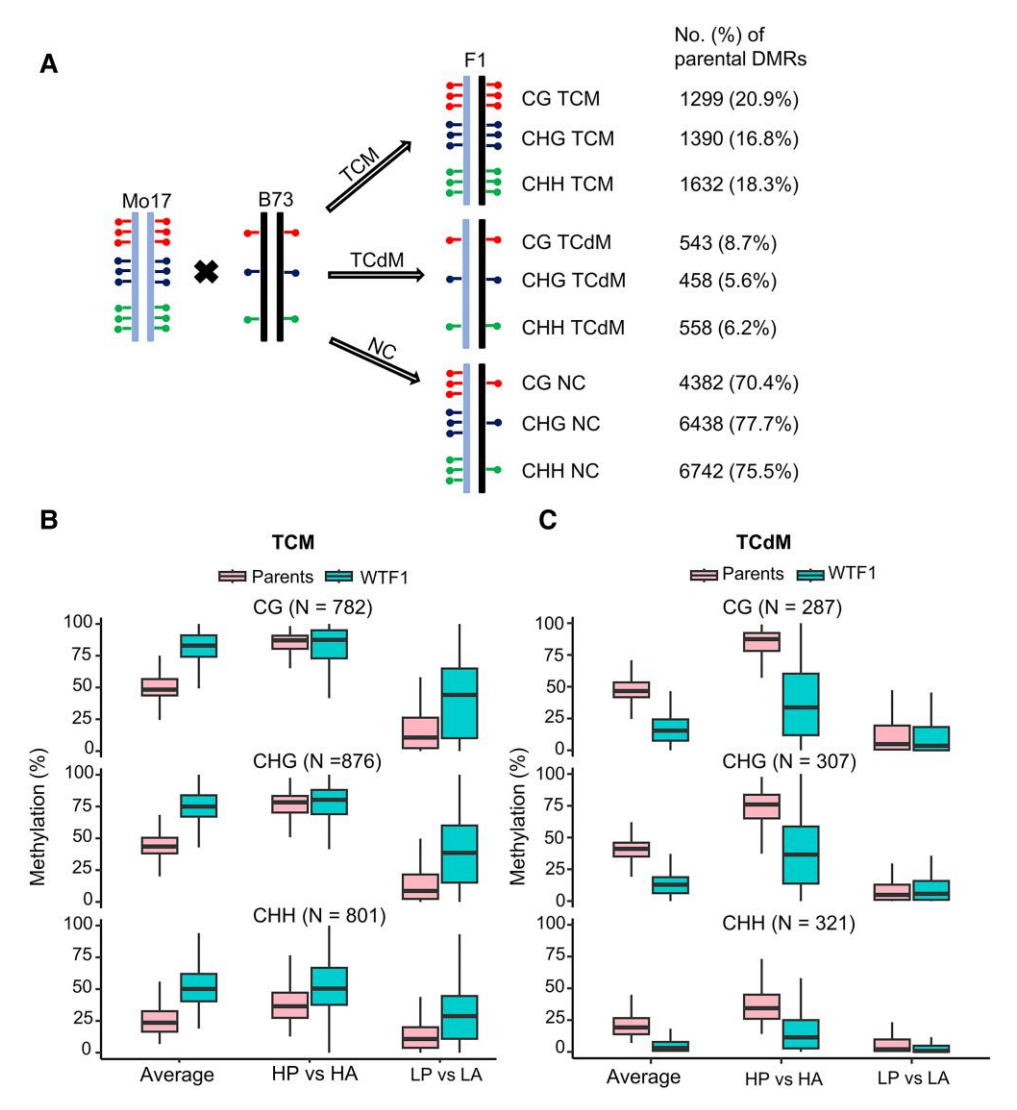


**Figure 3.** The levels of CHH methylation of both high- and low-parent alleles are increased at TCM DMRs in the F1 hybrids. **A)** Identification of TCM, TCdM, and unchanged (NC) DMRs between WTF1 and parents. **B)** Comparisons of CG, CHG, and CHH methylation at TCM DMRs in parents and WTF1. **C)** Comparisons of CG, CHG, and CHH methylation at TCdM DMRs in parents and WTF1. For **B)** and **C)**, the bottom and top boundaries of the box are the first and third quartiles, and the bold lines within individual boxes are the medians, which are referred to as the second quartiles. The ends of the whiskers (the lines) represent the minimum values and maximum values of the data. HP, high parent (parent with higher methylation); HA, high-parent allele in F1; LP, low parent (parent with lower methylation); LA, low-parent allele in F1. Average means the average between the 2 parents or between the 2 alleles in WTF1 and *mop1*F1. DMRs, differentially methylated regions; TCM, *trans*-chromosomal methylation; TCdM, *trans*-chromosomal demethylation.

DMRs (Fig. 2D), consistent with previous observations that CHH methylation is often found in mCHH islands immediately up- and downstream of genes (Gent et al. 2013; Li et al. 2015a). Out of the 13,307 CHH DMRs, 52% were located within or near genes, particularly 2 kb upstream and downstream of genes (43%), which was significantly higher than the values for CG (27%) and CHG (18%) in these regions (P < 0.0001,  $\chi^2$  test; Fig. 2E). Given that TEs are the primary targets of DNA methylation and maize genes are frequently adjacent to TEs (Li et al. 2015a; Erdmann and Picard 2020; Liu and Zhao 2023), we compared the different classes of TEs overlapping DMRs within the 2 kb flanking regions of genes. Not surprisingly given their distribution within

genomes, we found that terminal inverted repeat (TIR) DNA transposons were more enriched in CHH DMRs than they were in CG and CHG DMRs within 2 kb of genes (Fig. 2, E and F).

Next, we examined the methylation levels of these parental DMRs in the F1 hybrids. Following previously published studies, we compared the methylation levels of WTF1 to the MPV and classified changes as being a consequence of TCM, TCdM, or no change (NC; Fig. 3A; Zhang et al. 2016). A majority of parental DMRs (~75%) did not significantly change their methylation levels in the WTF1 hybrids, and most of these unchanged DMRs were in TEs and unclassified regions (Fig. 3A; Supplementary Fig. S5). However, when single

nucleotide polymorphisms (SNPs) were used to distinguish methylation in each of the 2 parental genomes, many of these NC DMRs (CG 53.8%, CHG 52.9%, and CHH 51.4%) in WTF1 were revealed to have lost methylation at the highparent allele and gained methylation at the low-parent allele, which resulted in no significant changes in overall methylation levels between the hybrids and parents, suggesting that methylation interaction still occurs in these NC DMRs (Supplementary Fig. S6). Of the remaining 25% parental DMRs that were significantly changed in F1 hybrids, 18.7% were TCM, and 6.8% were TCdM (Fig. 3A). We then compared allele-specific methylation levels of these regions between B73 and Mo17. Given that these 2 inbred genomes are highly polymorphic, we were able to compare allelespecific methylation at 2,459 (57%) of the TCM and 915 (59%) of the TCdM DMRs. At TCM DMRs, WTF1 had higher methylation levels at all 3 cytosine contexts (Fig. 3B). The increased methylation at CG and CHG in these wild-type F1 plants was primarily due to the increased methylation in the parental allele that had the lower level of methylation. In contrast, CHH methylation levels of both the high- and low-parent alleles were substantially increased in WTF1 at these TCM DMRs (Fig. 3B). At TCdM DMRs, the reduction of methylation was primarily due to the decreased methylation of the high-parent allele in all 3 cytosine contexts (Fig. 3C).

### Methylation of CHH TCM DMRs is dramatically reduced in the *mop1* mutant

To shed light on the effects of the loss of Mop1-dependent small RNAs at TCM and TCdM DMRs, we examined their methylation levels in mop1F1 mutant plants. Only 99 (8.6%) of 1,147 CG and 144 (11.2%) of 1,284 CHG TCM DMRs significantly changed their methylation levels in mop1F1 mutants. In contrast, methylation levels of 90.7% (1,031 out of 1,137) CHH TCM DMRs were significantly changed in mop1F1 (Fig. 4A). Consistent with our global analysis, the CHH DMRs that were significantly changed in mop1 were primarily located in the 2 kb flanking regions of genes (Supplementary Fig. S7). As expected, methylation of all the 3 sequence contexts at these TCM DMRs was largely reduced in mop1F1 mutants, particularly in the CHH context, in which the methylation level in mop1F1 plants was even lower than the low parent (Fig. 4B). This suggests that in these regions, but not the genome as a whole, the additional methylation in F1 wild-type plants is lost altogether. Not surprising, given that the methylation of TCdM DMRs was already very low, we did not observe significant changes in methylation at TCdM DMRs in the mop1F1 mutants (Fig. 4C).

Previous research has demonstrated that loss of methylation in mCHH islands results in additional loss of CG and CHG methylation (Li et al. 2015a). We found that out of the 118 CG DMRs that were significantly changed in *mop1*F1 mutants relative to their wild-type siblings, 37 (31.4%) were also CHG DMRs, but only 3 (2.5%) were CHH

DMRs. Similarly, only 32 (20.9%) and 9 (5.9%) of the CHG DMRs that were changed in *mop1* were CG and CHH DMRs, respectively. Out of the 1,048 *mop1*-affected CHH DMRs, 72 (6.7%) and 181 (17.3%) were also CG and CHG DMRs (Supplementary Table S4). A similar pattern was observed for the *mop1*-affected CHG DMRs, in which we detected changes in CG but no changes in CHH methylation. For *mop1*-affected CHH DMRs, we saw no change in CG but a substantial change in CHG (Fig. 4D). Together, these data suggest that the *mop1* mutation primarily prevents the methylation of CHH TCM DMRs, and that a loss of CHH methylation in *mop1* can result in additional loss of CHG, but not CG methylation.

# Small RNAs from 1 allele are sufficient to trigger methylation of the other allele at a majority of CHH TCM DMRs in F1 hybrids

Because small RNAs are the trigger for de novo DNA methylation (Matzke and Mosher 2014; Matzke et al. 2015), we next asked whether the difference in methylation during hybridization is caused by differences in small RNAs. We proposed 2 hypotheses with respect to siRNAs at the CHH TCM DMRs. As shown in Fig. 5A, in the first hypothesis, small RNAs are produced from 1 allele and trigger increases in methylation at the high-parent allele and de novo methylation in lowparent allele without triggering production of new, allelespecific small RNAs from that allele. In the alternative hypothesis, once methylation is triggered in the low-parent allele, it becomes competent to produce its own, allelespecific small RNAs, which may in turn act to enhance at the high-parent allele. To distinguish between these hypotheses, we performed small RNA sequencing from the same plants that were used for DNA methylation analysis (Supplementary Table S1). Because of the increase in the apparent number of 22-nt siRNAs in mop1 mutants caused by normalization following the loss of most 24-nt small RNAs in mop1 mutants, the small RNA values were adjusted to total abundance of all mature microRNAs following previously described protocols (Nobuta et al. 2008). As was expected, 24-nt siRNAs were the most abundant siRNAs in all the sequenced wild-type samples. Overall, despite the dramatic increase we observed in CHH methylation in the hybrids (Fig. 1B), no obvious differences in the quantity of small RNAs were observed between the WTF1 hybrids and the parents (Fig. 5B). The mop1 mutation substantially reduced 24-nt siRNAs, particularly in the mCHH island regions near TSSs and TTSs (Fig. 5B; Supplementary Fig. S8). Next, we compared 24-nt siRNAs generated from the high parent and low parent. We detected 24-nt uniquely mapped siRNAs in 795 CG (11.2% of the total), 700 CHG (7.7%), and 5,070 CHH (38.1%) parental DMRs. The average expression levels of 24-nt siRNAs in the high parent were 22.3, 18, and 66.9 RPKM at these CG, CHG, and CHH TCM DMRs, respectively, which were significantly higher than those observed in the low parent, which had 9, 8, and 36.9 RPKM 24-nt siRNAs,

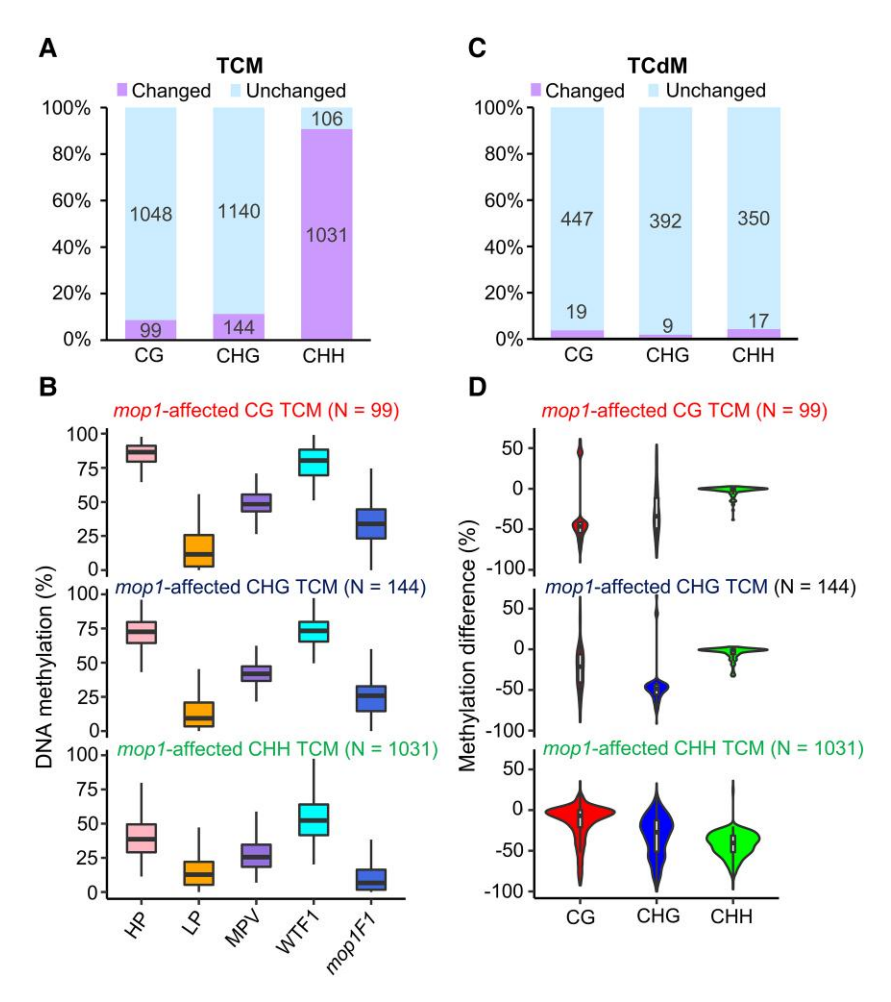


**Figure 4.** The *mop1* mutation primarily removes the methylation of CHH TCM DMRs. **A)** Number of CG, CHG, and CHH TCM DMRs affected by the *mop1* mutation. **B)** Comparison of methylation levels at the *mop1*-affected CG, CHG, and CHH TCM DMRs. **C)** Number of CG, CHG, and CHH TCM DMRs affected by the *mop1* mutation. **D)** Examination of the methylation changes in the other 2 cytosine contexts at the *mop1*-affected CG, CHG, and CHH TCM DMRs. The top panel shows the methylation changes in CHG and CHH sequence contexts for the 99 *mop1*-affected CG TCM DMRs. The middle panel shows the methylation changes in CG and CHH sequence contexts for the 144 *mop1*-affected CHG TCM DMRs. The bottom panel shows the methylation changes in CG and CHG sequence contexts for the 1,031 *mop1*-affected CHH TCM DMRs. For **B)** and **D)**, the bottom and top boundaries of the box are the first and third quartiles, and the bold lines within individual boxes are the medians, which are referred to as the second quartiles. The ends of the whiskers (the lines) represent the minimum values and maximum values of the data. HP, high parent (parent with higher methylation); LP, low parent (parent with lower methylation); MPV, the middle parent value; DMRs, differentially methylated regions; TCM, *trans*-chromosomal methylation; TCdM, *trans*-chromosomal demethylation.

respectively (Supplementary Fig. S9 and Table S5). This is also true for TCM, TCdM, and NC DMRs when analyzed separately (Supplementary Fig. S10).

To test whether the increase in methylation in WTF1 plants was due to an increase in 24-nt small RNAs, we compared the abundance of 24-nt siRNAs between WTF1 and the MPV. Although 24-nt siRNAs were increased at CHH TCM DMRs in WTF1 hybrids, this increase was not significant (Fig. 5C; Supplementary Fig. S10). We then analyzed allelespecific expressions of siRNAs in F1 hybrids. Because only uniquely mapped reads with SNPs can be used to assess the allele-specific expression of siRNAs and because the length (24 nt) of siRNAs is very short, we were able to obtain data from only 207 CHH TCM DMRs that had enough

information to compare allele-specific expression. There was no significant difference between the ratio of 24-nt siRNAs of the high-parent allele to the low-parent allele in F1 hybrids and that of the high parent to the low parent in the parents (Fig. 5D). Among these 207 CHH TCM DMRs, 53 had siRNAs expressed from only the high parent. Of these, 34 (64.2%) had siRNAs still produced from the high-parent allele in WTF1. Out of the remaining 154 CHH TCM DMRs, 104 expressed more siRNAs from the high parent, out of which 65 (62.5%) still had more siRNAs expressed from the high-parent allele compared to the low-parent allele in WTF1. These data suggest that the increased methylation at CHH TCM DMRs is not caused by an increase in siRNAs from the newly methylated allele, which favors the

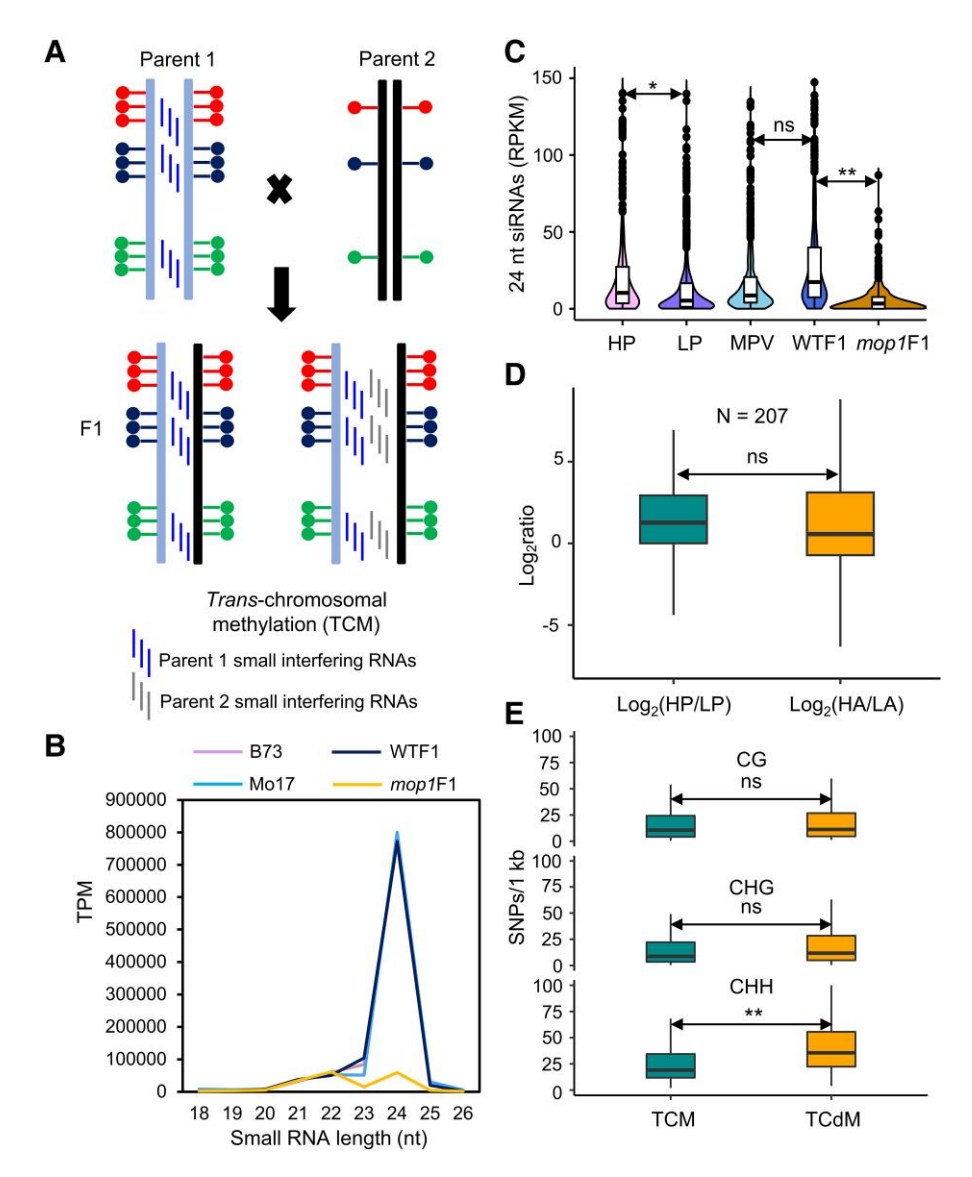


**Figure 5.** Small RNAs produced from 1 parent are sufficient to trigger new methylation of the other allele in hybrids. **A)** Two hypothetical models of small RNA biogenesis in F1 at CHH TCM. **B)** Expression values of small RNAs in parents, WTF1, and *mop1*F1. TPM, transcripts per million uniquely mapped reads. The small RNA values were adjusted to total abundance of all mature microRNAs following the previous research (Nobuta et al. 2008). **C)** The abundance of 24-nt siRNAs at the *mop1*-affected CHH TCM DMRs. HP, high parent (parent with higher methylation); LP, low parent (parent with lower methylation); MPV, the middle parent value; RPKM, 24-nt siRNA reads per kilobase (DMR length) per million uniquely mapped reads. **D)** Ratios of 24-nt siRNAs of the high parent to the low parent and of the high-parent allele to the low-parent allele at the *mop1*-affected CHH TCM DMRs. **E)** Number of SNPs between TCM and TCdM. For **C** to **E)**, the bottom and top boundaries of the box are the first and third quartiles, and the bold lines within individual boxes are the medians, which are referred to as the second quartiles. The ends of the whiskers (the lines) represent the minimum values and maximum values of the data. Individual data points beyond the whiskers are potential outliers, indicating values that deviate significantly from the overall pattern of the data. \*\*P < 0.01 and \*P < 0.05, Student's t test. ns, not significant; DMRs, differentially methylated regions; TCM, *trans*-chromosomal methylation; TCdM, *trans*-chromosomal demethylation.

hypothesis that small RNAs produced from 1 allele trigger methylation of the other allele in *trans*, but that the newly methylated allele is not itself a source of small RNAs.

RdDM triggered by small RNAs depends on the similarity of the small RNAs and their targets. Thus, the sequence variation between the 2 alleles may affect small RNA targeting and, ultimately, methylation. To test this, we compared the

SNPs between TCM and TCdM. As shown in Fig. 5E, no significant differences in SNP enrichment were observed when comparing TCM and TCdM at CG and CHG DMRs. In contrast, CHH TCdM DMRs had significantly more SNPs than did CHH TCM DMRs, suggesting that more genetic variation at CHH TCdM DMRs hinders targeting of 1 allele by small RNAs from the other allele.

#### CHH methylation of sequences flanking genes can be associated with either suppressed or enhanced expression of neighboring genes

Given the variation in DNA methylation we observed in the parental lines and F1 hybrids (Fig. 2), we compared the expression values of 51 genes involved in the RdDM pathway among these genotypes. We detected 8 RdDM genes differentially expressed between B73 and Mo17, all of which showed significantly higher expression in the Mo17 genome (Supplementary Fig. S11 and Table S6), which may contribute to the greater abundance of CHH methylation in the Mo17 genome (Fig. 2, B and C). In addition, we identified 6 RdDM pathway genes differentially expressed between the F1 hybrids and the MPV, all of which had higher expression in the F1 hybrids (Supplementary Fig. S11 and Table S7), suggesting that the RdDM pathway is more active in hybrids.

DNA methylation is generally associated with repression of transcription, particularly when the methylation is in the promoter regions of genes (Zilberman et al. 2007; Hollister and Gaut 2009; He et al. 2011). However, previous analysis of the maize methylome suggests that the reverse is true of CHH islands. One interpretation of this observation is that because CHH methylation is an active process that requires relatively open chromatin, increased gene expression may permit more efficient RdDM, resulting in higher levels of methylation (Gent et al. 2013; Li et al. 2015a). If this were the case, one would expect that allele-specific increases in expression in F1 plants would result in increased CHH methylation of TEs near those genes. Alternatively, it is possible that additional CHH methylation could, under some circumstance, result in decreased expression in F1 plants. To understand the relationship between CHH methylation and gene expression, we investigated the association between a subset of CHH TCM DMRs with expression of genes that flank them. As shown in Fig. 6A and Supplementary Fig. S12A, for the Mo17 CHH TCM DMRs, whose methylation is transferred from Mo17 to B73, if methylation suppresses gene expression, because the Mo17 parent has higher methylation, we expect the Mo17 allele to have a lower level of expression. After hybridization, if the B73 allele gains methylation, it would be expected to produce less transcript. If this is the case, we would expect to see the ratio of gene expression of the B73 to Mo17 alleles in the F1 hybrids to decrease relative to the ratio of expression of these alleles in the parents (Fig. 6A; Supplementary Fig. S12A, left panel). In contrast, if CHH methylation promotes gene expression, or if it responds positively to increased expression, we would predict an increase in the ratio of gene expression of the B73 to Mo17 alleles in F1 hybrids associated with a relative increase in expression of B73 (Fig. 6A; Supplementary Fig. S12A, right panel).

We focused on 442 Mo17 hyper-CHH DMRs with available data on allele-specific methylation in F1, 172 of which also had available allele-specific expression data, and then looked for genes whose allele-specific expression

changed significantly in F1 relative to the parents. Of the genes flanking the 172 Mo17 hyper-DMRs, 126 (73%) showed no significant change in relative expression. For 16 genes, the ratio of B73 to Mo17 expression was decreased, and for 31 genes, the ratio was increased in the F1 hybrids (Fig. 6B; Supplementary Fig. S12B), suggesting that CHH methylation can be associated with both suppressed and enhanced gene expression. Next, we asked whether variation in expression of genes is associated with variation in histone modifications. The 16 DMRs that were associated with suppressed gene expression were significantly more enriched for H3K27me3 and more depleted of H3K4me3 than the 31 DMRs that were associated with enhanced gene expression in B73 (Fig. 6C; Supplementary Fig. S12C; Ricci et al. 2019). The 31 genes that seemed to be enhanced by CHH methylation were typically longer, more highly expressed, and with higher gene body methylation than the 16 suppressed genes in Mo17 (Fig. 6D; Supplementary Fig. S12D).

Because the mop1 mutation results in reduced methylation in mCHH islands near genes (Li et al. 2015a; Zhao et al. 2021), we wanted to determine whether removal of methylation of the 16 and 31 DMRs in the mop1 mutant changed the expression of their flanking genes. We compared the methylation levels of CHH, CG, and CHG in the 16 and 31 CHH TCM DMRs. Because CG and CHG methylation at many of these 16 suppression-associated CHH DMRs was not available in the mop1 mutant, we were only able to examine methylation of the 31 enhanced-associated CHH DMRs in the mop1 mutant. As expected, in the mop1 mutant, CHH methylation was greatly reduced in these 31 DMRs, as was CG and CHG methylation (Fig. 6E), which echoes previous research (Li et al. 2015a). However, this reduction in CHH methylation did not have a significant effect on the expression of the 31 genes that seemed to be promoted by CHH methylation (Fig. 6F). These data suggest that variations in CHH methylation are a consequence, rather than a cause of variation in gene expression.

#### Most newly induced CG and CHG DMRs lose methylation, and most newly induced CHH DMRs gain methylation in F1 hybrids

In addition to examining changes in methylation of the parental DMRs, we also investigated the newly induced DMRs in F1 hybrids that were not differentially methylated in the parents. These newly induced DMRs can either gain or lose methylation at an allele relative to both parents (Supplementary Figs. S13, A and B, and S14, A and B). A total of 715 CG, 1,149 CHG, and 3,876 CHH new DMRs were identified (Supplementary Fig. S13). These newly induced DMRs were equally distributed as hyper- or hypo-DMRs relative to both the B73 and Mo17 genomes (Supplementary Fig. S13, C and D), which is different from the parental DMRs, most of which were enriched for CHH methylation in the Mo17 genome (Fig. 2B). The newly induced DMRs at CG and CHG sequence contexts largely overlapped with TEs

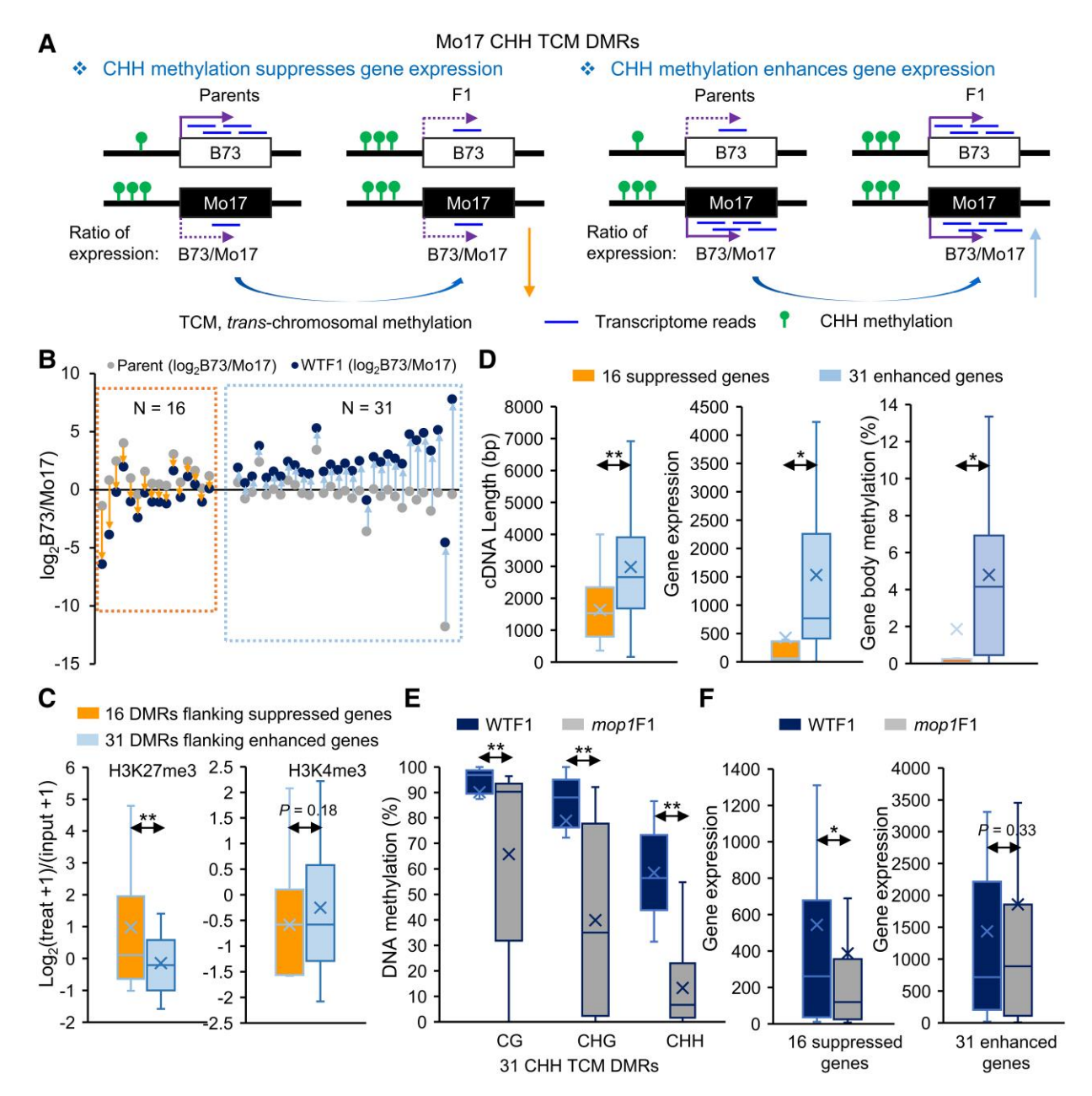


**Figure 6.** CHH methylation is associated with both suppressed and enhanced expression of their flanking genes. **A)** Two possible scenarios of the effects of CHH methylation on gene expression. Only examples of Mo17 CHH TCM DMRs are shown. The purple (horizontal) solid and dotted arrows indicate enhanced or suppressed expression of the gene in the parent or allele. The orange (downward) and blue (upward) arrows represent decreased and increased ratios of B73 to Mo17. **B)** Number of genes identified based on the models in **A)**. The ratios of expression values of B73 to Mo17 between the parents and WTF1 were used to distinguish the scenarios. **C)** Histone modification of 16 CHH TCM DMRs that are associated with the suppressed expression of flanking genes and 31 CHH TCM DMRs that are associated with the enhanced expression of flanking genes. **D)** Gene properties of the 16 suppressed and 31 enhanced genes. Introns were removed for measuring gene body methylation. **E)** Methylation changes in *mop1* mutants at the 31 CHH TCM DMRs that are associated with the enhanced expression of flanking genes. \*\*P < 0.01, Student's paired t = 0.01, Student's t = 0

(Supplementary Fig. S13, E and F), consistent with the fact that TEs are the most frequent targets of DNA methylation. Next, we compared the allele-specific methylation of these newly induced DMRs. Because the 2 parents were

methylated at the similar levels to those at these newly induced DMRs, we defined the high or low parent as the parental allele that was changed in the F1, so the low parent would be the allele whose methylation was reduced in the

F1. We found that the majority of newly induced CG (89%, 558 out of 627) and CHG (75%, 918 out of 1,231) DMRs followed the model in Supplementary Fig. S14B, in which 1 parental allele loses methylation in F1 hybrids (Supplementary Fig. S14D). Interestingly, the majority of newly induced CHH (92%, 2,959 out of 3,230) DMRs followed the model in Supplementary Fig. S14A, in which 1 parental allele gains methylation in F1 hybrids (Supplementary Fig. S14C), suggesting a distinction between CHH and CG and CHG methylation. We also compared the small RNAs at these newly induced CHH DMRs and did not observe any significant changes in small RNAs between the 2 parents that had similar methylation levels, or between the hybrids and parents (Supplementary Fig. S15).

### Initiation of the changes in the epigenetic state of CHH TCM loci does not require MOP1

We next wanted to determine whether the methylation or demethylation triggered in F1 can be maintained in subsequent generations. To test this, we backcrossed WTF1 (Mo17/B73;+/+) and mop1F1 (Mo17/B73;mop1/mop1)with B73 and obtained backcrossed (BC1) plants for WGBS (Fig. 1A). Because of recombination in the F1, each of the individual BC1 plants varied with respect to the proportion of B73 and Mo17 alleles they carried. Thus, each DMR from all 8 BC1 plants was determined for being either homozygous or heterozygous based on the SNPs between B73 and Mo17. DMRs containing recombination sites within them were excluded from the analysis due to their complexity. We first analyzed the overall methylation differences between WTF1 and WTBC1. To determine whether changes had been heritably transmitted, we set a cutoff for a lack of a change from WTF1 to WTBC1 as <10% change in methylation for CG and CHG and <5% for CHH methylation. We found that approximately 25% of CG and 26% of CHG TCM DMRs exhibited changes below this threshold in the WTBC1 plants, while 11% CHH TCM DMRs met the criteria. Interestingly, the CG (35%), CHG (44%), and CHH (38%) TCdM DMRs all had higher percentages of DMRs that did not change between F1 and BC1 (Supplementary Tables S8 and S9), suggesting that TCdM DMRs are more heritable.

To better understand the inheritance of newly acquired DNA methylation, we focused specifically on the inheritance of TCM DMRs. Given that all the sequenced BC1 plants were backcrossed individuals derived from the cross of F1 with B73, we separately analyzed B73 and Mo17 TCM DMRs. For B73 TCM DMRs (Figs. 7A and 8A; Supplementary Figs. S16A and S17A), in which the Mo17 allele gained new methylation in F1 (M\* in F1 in Figs. 7A and 8A), BC1 plants at these DMRs could be either homozygous or heterozygous for B73. Among the homozygous BC1 DMRs, all should have the native level of B73 methylation, as it was the Mo17 allele whose methylation was changed in the F1 at these DMRs. Similarly, BC1 DMRs that were heterozygous for B73 and the newly converted Mo17 allele (M\* in BC1 in Figs. 7A and 8A) would

be expected to remain hypermethylated due to the presence of the B73 allele in these plants (Figs. 7A and 8A). For CG and CHG methylation, this is what we observed. Methylation at these DMRs in all BC1 progeny (WTBC1 in Fig. 7, C and D), both homozygotes and heterozygotes, were at similar levels as the WTF1 (Fig. 7, C and D; Supplementary Fig. S16, C and D). Whether or not the F1 plant was *mop1* did not affect the heritability of the added methylation in these cases.

The heritability of CHH methylation was complicated by the fact that in each case, both alleles in the F1 had elevated methylation relative to the parents. BC1 B73 homozygous DMRs (WTBC1 in Fig. 8C) exhibited methylation levels similar to B73 (HP in Fig. 8C), rather than the WTF1 (Fig. 8C; Supplementary Fig. S17C), suggesting that the enhanced methylation in the F1 had been reduced in the BC1. In the BC1 heterozygous DMRs, the overall methylation level of WTBC1 was more similar to the MPV than the WTF1 (Fig. 8D; Supplementary Fig. S17C). This observation suggests that the globally elevated level of methylation at DMRs in the F1 is a consequence of the hybridization and not just a TCM interaction between each pair of alleles, and that the elevated levels of methylation at Mo17 in the F1 were not heritable.

In terms of heritability, the Mo17 TCM DMRs (Figs. 7B and 8B; Supplementary Figs. S16B and S17B) are more informative. In these cases, the B73 allele (B\* in F1 in Figs. 7B and 8B) became hypermethylated due to the presence of the Mo17 allele in the F1. The BC1 plants could be either homozygous for B73 at these DMRs, in which 1 epiallele (B\* in F1 in Figs. 7B and 8B) would remain more methylated if the change at B73 in the F1 was heritable, or heterozygous for Mo17 and B73, in which the B73 allele from the backcrossed parent would be expected to acquire enhanced methylation due to the presence of the Mo17 allele in the BC1 generation. Thus, if the change in the B73 in the F1 (B\*) was heritable, we would expect to see methylation in BC1 homozygous DMRs similar to the MPV. In the heterozygotes, we would expect a similar average level of methylation as was observed in the F1 (Fig. 7B).

For CG and CHG methylation at the Mo17 TCM DMRs, BC1 B73 homozygous DMRs (WTBC1 in Fig. 7E) were similar to the MPV of B73 and Mo17 (Fig. 7E; Supplementary Fig. S16, E and F), suggesting that changes caused in the F1 plants at B73 (B\*) were heritably transmitted to the next generation. In contrast, BC1 heterozygous DMRs (WTBC1 in Fig. 7F), which should resemble the F1 because they carried both B73 and Mo17, were also at the MPV (Fig. 7F; Supplementary Fig. \$16, E and 6F). This suggests that the increase in methylation in B73 due to the presence of Mo17 observed in the F1 did not occur in BC1, suggesting that the effects we observed in F1 are not simply due to allelic interactions but a consequence of the hybridization. For CHH methylation at the Mo17 TCM DMRs, BC1 plants (WTBC1 in Fig. 8, E and F), whether homozygous and heterozygous for a given allele, exhibited methylation levels similar to the MPV, rather than the elevated methylation observed in the F1 (Fig. 8, E and F; Supplementary Fig. S17D). This indicated that CHH

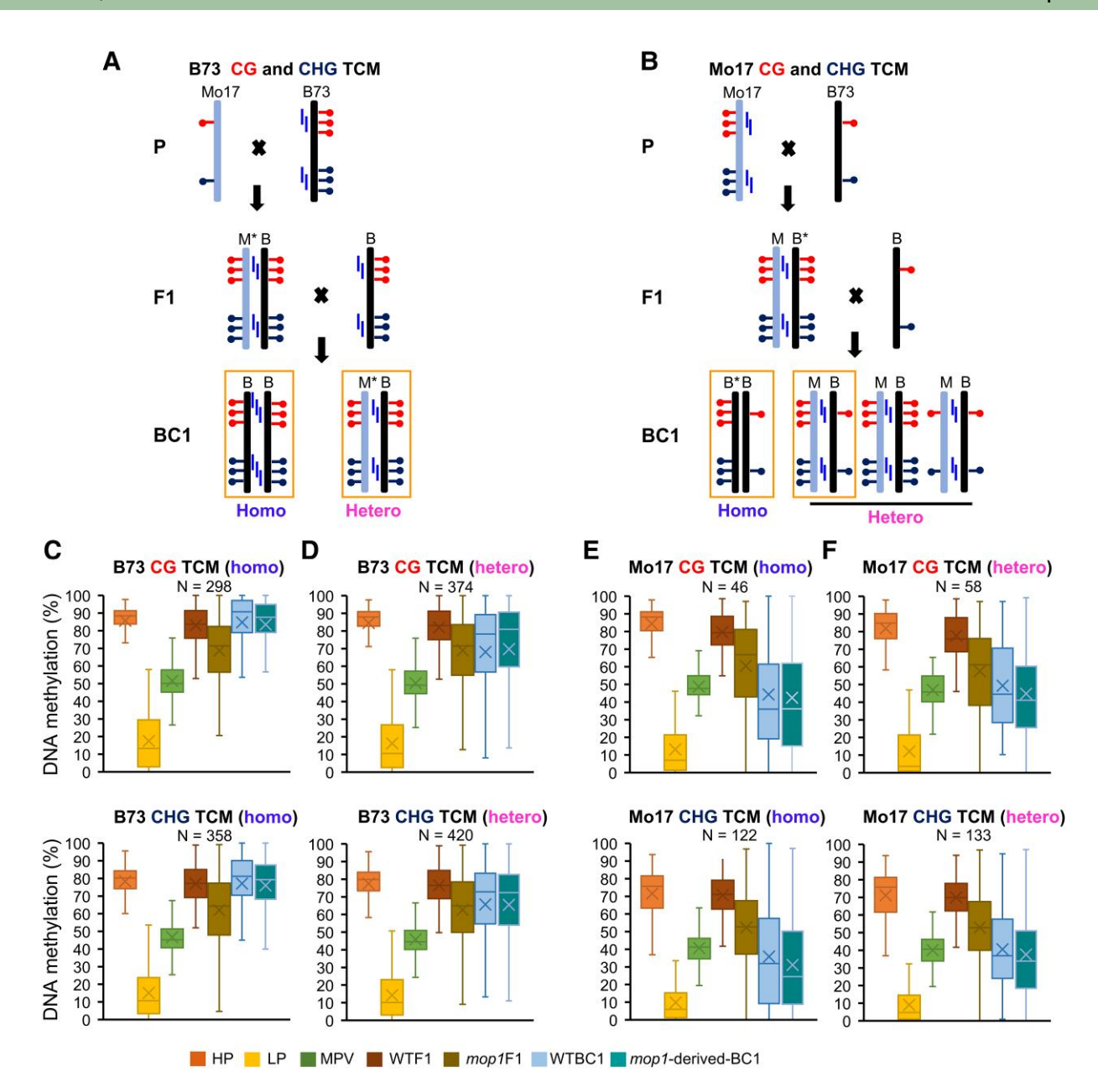


**Figure 7.** Newly triggered methylation at CG and CHG TCM DMRs in F1 plants is maintained in the next generation. **A)** Hypothetical model of maintenance of B73 CG and CHG TCM DMRs. The asterisks (M\*) denote the newly converted (methylated) allele. M, Mo17; B, B73. The blue vertical bars near each allele represent siRNAs, and the orange boxes indicate the models supported by the data in **C** to **F)**. **B)** Hypothetical model of maintenance of Mo17 CG and CHG TCM DMRs. The asterisks (B\*) denote the newly converted (methylated) allele. M, Mo17; B, B73. **C)** Methylation changes of homozygous B73 CG and CHG TCM DMRs. **D)** Methylation changes of heterozygous B73 CG and CHG TCM DMRs. **E)** Methylation changes of homozygous Mo17 CG and CHG TCM DMRs. **F)** Methylation changes of heterozygous Mo17 CG and CHG TCM DMRs. For **C** to **F)**, the bottom and top boundaries of the box are the first and third quartiles, and the bold lines within individual boxes are the medians, which are referred to as the second quartiles. The ends of the whiskers (the lines) represent the minimum values and maximum values of the data. DMRs, differentially methylated regions; TCM, *trans*-chromosomal methylation; Homo, homozygous; Hetero, heterozygous; WTBC1, Mo17/B73; +/+ × B73; *mop1*-derived BC1, Mo17/B73;*mop1/mop1* × B73.

methylation added to the B73 allele was inherited in BC1, and the presence of the Mo17 allele did not trigger new methylation in B73 in the BC1 generation.

To determine whether the initiation of TCM requires the presence of MOP1, we also looked at BC1 derived from mop1F1 mutants (Mo17/B73; $mop1/mop1 \times B73$ ). Our

expectation was that if the transfer of heritable methylation requires MOP1, backcrossed progeny of *mop1*F1 would not carry that methylation if they only carried the modified allele. The most informative class was the B73 homozygous progeny of Mo17 TCM DMRs that had shown evidence of heritable changes in methylation of the B73 allele (Figs. 7E

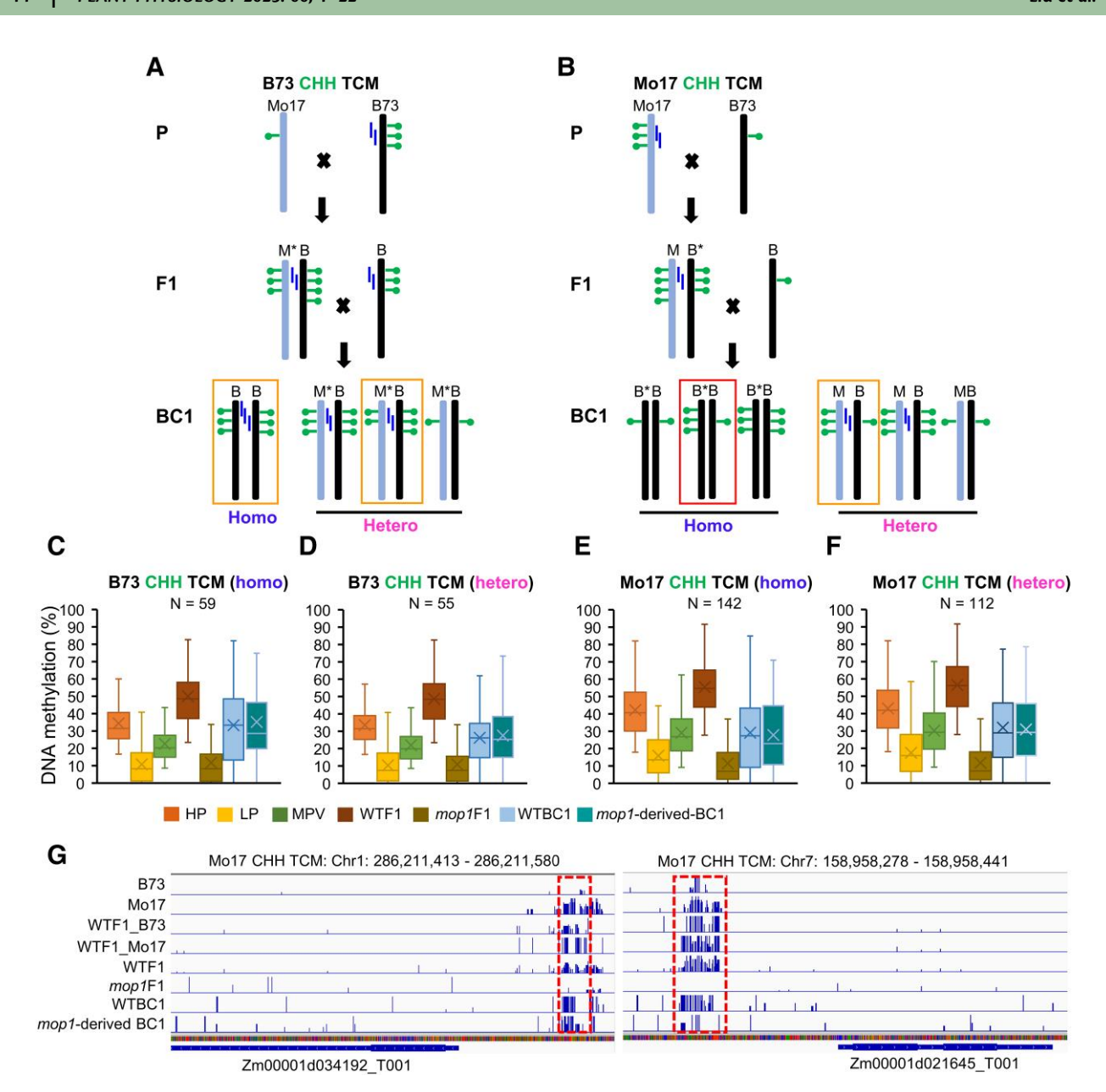


**Figure 8.** Initiation of the changes in the epigenetic state of *trans*-chromosomal CHH methylation in maize does not require MOP1. **A)** Hypothetical model of maintenance of B73 CHH TCM DMRs. The asterisks (M\*) denote the newly converted (methylated) allele. M, Mo17; B, B73. The blue vertical bars near each allele represent siRNAs. **B)** Hypothetical model of maintenance of Mo17 CHH TCM DMRs. The asterisks (B\*) denote the newly converted (methylated) allele. M, Mo17; B, B73. The orange (from left to right, the box numbered 1, 2, and 4) and red (the box numbered 3) boxes indicate the models supported by the data in **C** to **F)**. **C)** Methylation changes of homozygous B73 CHH TCM DMRs. **D)** Methylation changes of heterozygous B73 CHH TCM DMRs. **E)** Methylation changes of homozygous Mo17 CHH TCM DMRs. **F)** Methylation changes of heterozygous Mo17 CHH TCM DMRs. **G)** Distribution and methylation levels of 2 examples of Mo17 CHH TCM DMRs. The red dashed boxes highlight the DMR in each example. For **C** to **F)**, the bottom and top boundaries of the box are the first and third quartiles, and the bold lines within individual boxes are the medians, which are referred to as the second quartiles. The ends of the whiskers (the lines) represent the minimum values and maximum values of the data. DMRs, differentially methylated regions; TCM, *trans*-chromosomal methylation; Homo, homozygous; Hetero, heterozygous; WTBC1, Mo17/B73;+/+ × B73; *mop1*-derived BC1, Mo17/B73;*mop1/mop1* × B73.

and 8E). For CG and CHG TCM methylation, we found that although the *mop1* mutant had a minor effect on methylation in the F1, it had no effect on the heritability of CG and CHG methylation that had been added to the B73 allele (B\*) in F1 Mo17 TCM DMRs (Fig. 7E). In contrast, for CHH methylation, the substantial additional CHH methylation

that was added in the F1 generation (WTF1 in Fig. 8E) at these Mo17 CHH TCM DMRs was not transmitted to the next generation of wild-type hybrids (WTBC1 in Fig. 8E). However, wild-type progeny of *mop1*F1 mutant plants (*mop1*-derived BC1 in Fig. 8E) that had been nearly devoid of CHH methylation in the F1 (*mop1*F1 in Fig. 8E, 2 examples

in Fig. 8G) was competent to reestablish CHH methylation to the MPV level (Fig. 8, B [red left box], E, and G), suggesting that the epigenetic states at those alleles retained enough information for CHH methylation to be targeted back to them in the wild-type BC1 progeny.

Together, these data suggest that methylation or demethylation triggered by hybridization can be maintained in the next generation, but that heritability varies depending on the sequence context of the methylated cytosines, and whether new methylation or demethylation is being transmitted. Our data also show that the elevated methylation we observed in F1 is likely a result of hybridization, rather than simple interaction between alleles.

#### **Discussion**

In this study, we used hybrids as a model system to understand the initiation and maintenance of DNA methylation in maize, with a special focus on CHH methylation, which is abundant in plants, but whose functions are still poorly understood. Our analyses revealed that CHH methylation had some unique features compared to CG and CHG methylation in maize. These include global increases in CHH methylation, local increases at both high- and low-parent alleles at TCM DMRs, and its association with both increases and decreases in flanking gene expression. Notably, we observed an overall reduction in CHH methylation levels in the backcrossed individuals relative to F1 plants (Fig. 8). This suggests that the high levels of CHH methylation at individual DMRs in F1 plants are unlikely to be a consequence of trans interaction between these alleles alone and are thus more likely to be a manifestation of the global effects of hybridization, a conclusion supported by the observations that the inclusion of 25% Mo17 chromosomal material in each of the BC1 individuals is not associated with increases in CHH methylation at these DMRs.

It is worth noting that the 2 sequenced parental lines (B73; +/+ and Mo17;+/+) were not the actual parents of the F1 plants, both of which were heterozygous for *mop1*. Thus, it is possible that the elevated levels of CHH methylation we observed in the F1 plants were already present in the *mop1* heterozygous parents. However, we consider this unlikely because all the BC1 progeny we examined was also heterozygous for *mop1* but did not exhibit an elevated level of CHH methylation. It is also possible that those elevated levels of CHH methylation were a mapping artifact. We suggest this is unlikely because these issues would not be expected to only include CHH sites. Further, we saw no substantial increase in methylation in the synthetic F1 (Fig. 1B; Supplementary Figs. S1 and S2).

CHH methylation buffers the transcriptional activation of TEs near genes during hybridization Hybridization brings together 2 divergent genomes into 1 nucleus, which can induce rapid genomic and epigenomic

changes, including gain or loss of DNA fragments, alteration of expression of TEs and genes, changes in splicing sites, activation of endogenous retroviruses, and epigenetic reprogramming (Ishikawa and Kinoshita 2009; Regulski et al. 2013; Qin et al. 2021). It has been hypothesized that hybridization could induce a "genomic shock" that leads to the mobilization of TEs (McClintock 1984). However, evidence for this is mixed and varies between species. Most reports suggest that upregulation of TEs is not a general phenomenon but that some specific TEs may change their expression level upon hybridization, such as the upregulation of ATHILA in the crosses of A. thaliana and Arabidopsis arenosa (Josefsson et al. 2006; Gobel et al. 2018). In our study, we observed a genome-wide increase in CHH, but not CG or CHG methylation following hybridization (Fig. 1B). Based on this result, we hypothesize that CHH methylation may buffer the global effects of hybridization on transcriptional activation of TEs near genes in maize by transferring silencing information in the form of small RNAs from 1 genome to the other, resulting in the dramatic increases in CHH de novo methylation observed in the F1 plants.

The lack of evidence for the production of new siRNAs from the target loci suggests that in many cases, this methylation is often transient, as is evidenced by the reduced heritability of CHH, CG, and CHG methylation in BC1 plants (Figs. 7 and 8). Our analysis of gene-adjacent TEs in wild-type and mutant F1 plants reveals that the cause of the increases in CHH methylation observed in F1 hybrids varies depending on location. As has been observed previously (Li et al. 2015a), the sharp increase in CHH methylation at the proximal portion of TEs near genes that are referred to as mCHH islands is dramatically reduced in the mop1 mutant (Fig. 1, C and D). The substantial increase in CHH methylation in these regions observed in F1 wild-type plants are largely eliminated in the mutant as well, resulting in an overall level of CHH methylation in the F1 mop1 mutants that is lower than both parents. That is not true in the body of gene-adjacent TEs, where CHH methylation actually increases in the F1 mop1 mutant. At the distal edge of those TEs, although the methylation added in the F1 plants is lost, the preexisting methylation in the parents is not. In the region distal to the TEs, only a subset of the additional CHH added in the F1 plants is dependent on Mop1 (Fig. 1D). This pattern is characteristic of the vast majority of the chromosomes outside of the gene-rich distal ends. Together, these data suggest that the global increase in CHH methylation observed in F1 hybrids varies with respect for a requirement for classical RdDM, with the large increases in CHH islands being the only region entirely dependent on it.

### Small RNAs play a role in transient trans-chromosomal CHH methylation

An overall reduction of 24-nt siRNAs following hybridization has been documented in a number of plant species including maize (Groszmann et al. 2011; Barber et al. 2012;

Greaves et al. 2016). However, in our analyses, we focused on 24-nt siRNAs specifically at TCM DMRs and observed no significant difference in the abundance of 24-nt siRNAs between hybrids and the MPV of parents (Fig. 5C), as has been observed in Arabidopsis (Zhang et al. 2016). This suggests that the increase in TCM DMR methylation in the lowparent allele is not due to a difference in the quantity of small RNAs. A detailed look at 53 CHH TCM DMRs that had 24-nt siRNAs produced only in 1 parent showed that 34 (64%) of them had only siRNAs derived from the initially methylated parental allele (Supplementary Table S5), despite the fact that both alleles now had CHH methylation. Given that the precursor transcript of 24-nt siRNAs is produced by Pol IV (Matzke and Mosher 2014; Matzke et al. 2015), this observation suggests that Pol IV in these F1 plants is only active at 1 of the 2 methylated alleles. It is unclear as to why Pol IV does not appear to recognize the newly methylated allele.

Our data also showed that CHH TCdM DMRs had significantly higher genetic variation than TCM DMRs, as has been noted previously (Fig. 5E; Zhang et al. 2016). Given that RdDM relies on similarity between small RNAs and their targets, this may explain the reduction of methylation at TCdM DMRs. Small RNAs from the high-parent allele may be too divergent to target the low-parent allele to trigger methylation. However, it is unclear why the methylation of the highparent allele is also reduced in the TCdM DMRs. One hypothesis that has been suggested is that small RNAs from the high-parent allele can interact with the low-parent allele unproductively, which dilutes siRNA concentration at the donor allele, which in turn weakens the methylation of the donor allele (Zhang et al. 2016). However, we do not believe this is the general mechanism for TCdM, as in our study, 41.3% of these TCdM DMRs do not have any polymorphisms (Fig. 3). It has been proposed that TCdM may be regulated by distal factors (Kakoulidou and Johannes 2023). These distal factors have also been used to explain newly induced DMRs. In this so-called "TCM proximity model," a gain of methylation at TCM DMRs during hybridization spreads into flanking regions, resulting in the increased methylation in F1 at those regions, in which parental alleles have the similar methylation state (Kakoulidou and Johannes 2023). However, we tested this model in our data set and did not find evidence supporting this hypothesis.

### De novo CHH methylation is associated with both increased and decreased expression of flanking genes

It has been proposed that mCHH islands in maize are the boundaries between highly deep heterochromatin and more active euchromatin to reinforce silencing of TEs located near genes rather than to protect the euchromatic state of the genes (Gent et al. 2013; Li et al. 2015a; Martin et al. 2021). Our study is an ideal model to test this hypothesis because we can examine the effects of presence and absence of mCHH islands on the expression of the same gene in *cis* and in *trans*. For example, as shown in Fig. 6A, a gene in the parent

B73 does not have CHH methylation in the promoter region, but obtains methylation after hybridization, which we hypothesize is triggered in trans by small RNAs generated from the Mo17 allele. We demonstrated that out of the 47 CHH TCM DMRs in Mo17 (Mo17 mCHH islands), 16 (34%) were associated with suppressed gene expression, and 31 (66%) were associated with enhanced gene expression (Fig. 6B), indicating that a gain of CHH methylation in their promoter regions may actually enhance their expression. Alternatively, it may be that gene properties and chromatin states may dictate the relationship between CHH islands and their flanking genes. The 31 genes whose expression appeared to be promoted by CHH methylation were generally longer, expressed higher, and with more gene body methylation than the 16 genes that seemed to be suppressed by CHH methylation (Fig. 6D). These data suggest that more active genes tend to harbor "positive mCHH islands," and lowly expressed genes more likely have "negative mCHH islands," which were significantly enriched for the repressive histone mark H3K27me3 and were depleted with the active mark H3K4me3 (Fig. 6C). We hypothesize that it is the repressive histone mark in the promoter regions that suppresses the expression of flanking genes rather than the mCHH islands. Given this assumption, removal of these islands would not have substantial effects on flanking gene expression. However, removal of DNA methylation may result in increase of H3K27me3 given that the activity of Polycomb-repressive complex 2, which is involved in catalyzing H3K27me3, is generally antiassociated with DNA methylation and likely functions after DNA demethylation (Rodrigues and Zilberman 2015; Batista and Kohler 2020). This probably explains why we observed these 16 genes with "negative mCHH islands" significantly reduced their expression in mop1 mutants (Fig. 6F). In contrast, the expression of the 31 genes with "positive mCHH islands" was upregulated in the mop1 mutant although not significantly (Fig. 6F), which supports the hypothesis that mCHH islands do not prevent the spread of heterochromatin silencing of genes (Li et al. 2015a). Rather, these "positive mCHH islands" act as a border to prevent the spread of euchromatin into flanking sequences because loss of the mCHH islands in the mop1 mutant is accompanied by additional loss of CG and CHG methylation (Fig. 6E; Li et al. 2015a).

### Initiation of the changes in the epigenetic state of CHH TCM loci does not rely on RdDM

One of the most remarkable findings is that while increased CHH methylation in F1 plants did require MOP1, changes in the epigenetic state of these CHH TCM DMRs did not require a functional copy of this gene. This observation is supported by Fig. 8, B (red left box) and E, where it is evident that despite the removal of CHH methylation due to the *mop1* mutation in the F1 plants, the methylation is reestablished in the BC1 progeny, even in the absence of small RNAs in their parents (as indicated by homozygous B73 in Fig. 8, B and E).

We can imagine 2 possible explanations for this observation. One is that the methylation at a given CHH DMR in Mo17 is driven in trans by small RNAs produced at 1 or more other loci in the Mo17 background. When the B73 allele of that locus is exposed to the Mo17 background in the F1 plants, it is targeted by those trans-acting small RNAs. Because those small RNAs required MOP1, F1 mop1 mutant plants are missing CHH methylation at those loci. However, in the BC1 plants, which are heterozygous for mop1, both alleles are again targeted, and both alleles are methylated. Although formally possible, we find this less likely because all of the Mo17 DMRs were uniformly remethylated even following the loss of an average of 50% of the Mo17 genome in these plants. A second possibility is that the B73 allele (B\* in Fig. 8B) was converted in trans via a process that does not require MOP1-dependent small RNAs derived from the Mo17 allele. A recent study investigated the transgenerational de novo DNA methylation of TEs after the loss of silent marks and demonstrated that the histone H2A. variants (e.g. H2A.W) may enable cells to retain a memory of where to reintroduce H3K9me2 and CHG(H) methylation (To et al. 2020). Similarly, in maize, the loss of mop1 results in the immediate loss of DNA methylation in all 3 sequence contexts at silenced MuDR elements, but a heritable silenced state is retained at this transposon, and methylation is restored in mop1 wild-type progenies (Guo et al. 2021). It is possible that despite the absence of both small RNAs and DNA methylation at those loci in mop1F1 plants, the presence of histone modifications or histone variants such as H2A.W might persist at those alleles, which are inherited to the next generation and could potentially facilitate the reestablishment of CHH methylation in the BC1 progeny. What is distinctive about our observations is that it suggests that not just maintenance but initiation of changes in the epigenetic state (likely in the form of histone modification) is not dependent on RdDM. It would be interesting to investigate the levels of H2A.W and H2A.Z as well as some other histone such as H2K9me2 modifications in wild-type F1, mutant F1, parents, and BC1 progeny. This investigation would not only shed light on the potential involvement of these histone variants and modifications in orchestrating the observed epigenetic alterations but also provide insights into the mechanisms underlying hybrid vigor.

#### Materials and methods

#### Genetic material construction and tissue collection

The *mop1* heterozygous maize (*Z. mays*) plants in the Mo17 background were crossed with the *mop1* heterozygous plants in the B73 background (Mo17;*mop1-1*/+ × B73;*mop1-1*/+) to generate F1 hybrid *mop1* mutants (Mo17/B73;*mop1*/*mop1*) and their hybrid wild-type siblings (Mo17/B73;+/+; Fig. 1A). The *mop1* mutation was introgressed into the B73 and Mo17 backgrounds for at least 7 generations. The F1 plants

and the 2 parental lines (B73 and Mo17) were grown in the Ecology Research Center at Miami University (Oxford, Ohio), and 5 to 7 cm immature ears were collected for the subsequent WGBS, RNA sequencing, and small RNA sequencing with 2 biological replicates for all samples examined.

#### Analysis of WGBS data

DNA was isolated from the 5 to 7 cm immature ears of the 2 parents (B73 and Mo17), WTF1 (Mo17/B73;+/+), and mop1F1 (Mo17/B73;mop1/mop1) using the modified CTAB method. The quality of DNA was examined by NanoDrop. Library construction and subsequent WGBS were performed by Novogene. The raw reads were quality controlled by FastQC. The remaining clean reads from B73, WTF1, and mop1F1 were mapped to the B73 reference genome (v4) using Bismark under following parameters (-I 50, -N 1; Krueger and Andrews 2011; Jiao et al. 2017). To map the Mo17 reads, we generated a pseudo-Mo17 genome by taking the B73 reference sequences and replacing the nucleotides where a SNP identified by the maize Hapmap3 project was present between the 2 inbreds (Bukowski et al. 2018). The clean reads from the Mo17 plants were aligned against the pseudo-Mo17 genome. Given that treatment of DNA with bisulfite converts cytosine residues to uracil, but leaves 5-methylcytosine residues unaffected, SNPs of C to T and G to A (B73 to Mo17) were excluded from the analysis when considering the B73 allele, and SNPs of T to C and A to G (B73 to Mo17) were excluded from the analysis when considering the Mo17 allele (Li et al. 2023). We kept the reads with perfect and unique matches for the 2 parents and allowed 1 mismatch for the hybrids. PCR duplicates were removed using Picardtools. Additional packages including Bismark methylation extractor, bismark2bedGraph, and coverage2cytosine under Bismark were used to extract the methylated cytosines and to count methylated and unmethylated reads (Liu et al. 2021; Yin et al. 2022).

#### Identification of DMRs between parents

To identify DMRs between parents, we first filtered out the cytosines with less than 3 mapped reads (Xu et al. 2020). Next, the methylation level of each cytosine was determined by the number of methylated reads out of the total number of reads covering the cytosine (Schultz et al. 2012; Zhao et al. 2017). The software "metilene" was used for DMR calling between the 2 parents B73 and Mo17 (Juhling et al. 2016). Specially, a DMR was determined as containing at least 8 cytosine sites with the distance of 2 adjacent cytosine sites <300 bp and with the average methylation differences in CG and CHG > 0.4 and in CHH > 0.2 between the 2 parents (Xu et al. 2020). These DMRs were further filtered by the estimated false discovery rates (FDRs) using the Benjamini-Hochberg method (Zhang et al. 2016). We only kept FDRs <0.01 for CG and CHG DMRs and <0.05 for CHH DMRs (Xu et al. 2020).

#### Control analysis for methylome data

To address the concerns regarding the lower mapping rates of Mo17 reads due to the use of the pseudo-Mo17 genome, we conducted a parallel analysis using the recently released Mo17 genome sequences as the reference and generated a pseudo-B73 genome (Chen et al. 2023). To identify the SNPs between B73 and the authentic Mo17 genome, we first downloaded raw reads from B73 (Hufford et al. 2021), performed read trimming using Trimmomatic v0.36 (Bolger et al. 2014), and subsequently aligned them to the authentic Mo17 genome using BWA mem (Li and Durbin 2009). Subsequently, SNPs were identified using HaplotypeCaller in the Genome Analysis Toolkit (GATKv4.1, http://www. broadinstitute.org/gatk) with default parameters. A pseudo-B73 genome was then generated by substituting the nucleotides at SNP positions with those from the authentic Mo17 sequences. Next, we mapped the WGBS reads from both Mo17 and B73 plants to the authentic Mo17 genome and the pseudo-B73 genome, respectively, following the Bismark pipeline (Krueger and Andrews 2011). DMRs between the 2 parent lines, B73 and Mo17, were identified using metilene (Juhling et al. 2016), as described above. The results are shown in Supplementary Fig. S4.

Another control analysis involved creating a synthetic F1 hybrid methylome by combining an equal number of Mo17 and B73 WGBS reads. We performed the same analysis for the synthetic F1 hybrid methylome as for the authentic F1 hybrids. The results are illustrated in Fig. 1B and Supplementary Figs. S1 and S2.

#### Determination of TCM and TCdM in WTF1

To determine the methylation patterns of the parental DMRs in WTF1, we first calculated the methylation levels at the parental DMRs in WTF1. Only DMRs with available data in all the samples were included in the analysis. Fisher's exact test was used to compare the methylation levels of WTF1 to the MPV (the average methylation of the 2 parents), and the estimated FDRs were generated to adjust *P* values using the Benjamini–Hochberg method (Zhang et al. 2016). DMRs with an FDR <0.05 between WTF1 and the MPV were retained as significantly changed DMRs during hybridization. These DMRs were classified into TCM, which has a significantly higher level of methylation in WTF1 than the MPV, and TCdM, which has a significantly lower level of methylation in WTF1.

To further determine whether the TCM and TCdM were affected by *mop1* mutation, we first calculated the methylation levels of *mop1*F1 at TCM and TCdM DMRs. For CG and CHG TCM and TCdM, DMRs with the changes in methylation levels between *mop1*F1 and WTF1 <-0.4 or >0.4 were considered as significantly affected by the mutation. For CHH TCM and TCdM, DMRs with the changes in methylation levels <-0.2 or >0.2 were considered as significantly changed in the mutants.

#### Identification of the newly induced DMRs in WTF1

To identify the newly induced DMRs in WTF1 that are not differentially methylated in the parents, we used mpileup in the samtools package and SNPs between B73 and Mo17 to obtain the allele-specific reads from WTF1 (Danecek et al. 2021). Next, these allele-specific reads were used to calculate methylation levels as described above, and "metilene" was used for DMR detection between the 2 alleles in WTF1 (Juhling et al. 2016). The same cutoffs are used for defining new DMRs as for the detection of parental DMRs. The methylation levels at these newly induced DMRs were further compared between the 2 parents using Fisher's exact test (FDR <0.05). The DMRs that have similar methylation levels between the 2 parents but exhibit significantly different methylation levels between the 2 alleles in WTF1 were defined as new DMRs. The illustration is shown in Supplementary Fig. S13, A and B.

#### Analysis of the inheritance of TCM and TCdM in BC1

We backcrossed WTF1 (Mo17/B73;+/+) and mop1F1 (Mo17/ B73;mop1/mop1) with B73 (Mo17/B73; $+/+ \times$  B73 and Mo17/ B73; $mop1/mop1 \times B73$ ) to generate the BC1 generation. We collected 5 to 7 cm immature ears from 8 WTBC1 plants and 8 mop1-derived-BC1 plants for WGBS (Fig. 1A). The methylation analysis for BC1 is the same as that for parents and WTF1. Next, we compared the methylation levels at the TCM and TCdM DMRs among WTBC1, mop1-derived-BC1, WTF1, mop1F1, and parents. The "intersect" function in BEDTools was used to access all the cytosines in BC1 that are at the TCM and TCdM DMRs, and these cytosines were used to calculate the average methylation levels across all the BC1 individuals in those regions. As shown in Figs. 7 and 8, because we only sequenced the BC1 individuals derived from the backcrosses of F1 and B73, we separated B73/B73 homozygous and B73/Mo17 heterozygous genotypes at each TCM DMR in BC1 using samtools mpileup and the SNPs between B73 and Mo17 (Bukowski et al. 2018; Danecek et al. 2021), same as what we did for the determination of allele-specific reads in F1.

### Distribution analysis of DMRs in different genomic locations

To classify the DMRs in different genomic locations, we compared the locations of the DMRs with gene and TE annotations, which were downloaded from MaizeGDB, https://www.maizegdb.org/, using intersect function in BEDTools (Quinlan and Hall 2010). If 1 DMR is dropped to 2 different types of annotation, we followed the order gene bodies, 2 kb upstream of genes, 2 kb downstream of genes, TEs, and unclassified regions. DMRs in the 2 kb up- and downstream regions of genes were further separated into those with and without TEs depending on whether it overlaps a TE insertion in the 2 kb flanking regions.

#### Analysis of small RNA-seq data

The same genetic materials for B73 and Mo17, WTF1, and mop1F1 were used for small RNA sequencing with 2 biological replicates. The raw reads were quality controlled by FastQC. The clean reads were aligned against the Rfam database (v14.6) to remove rRNAs, tRNAs, snRNAs, and snoRNAs (Yin et al. 2022). The remaining reads with the length of 18 to 26 nt were retained for further mapping to the genomes. The reads from B73, WTF1, and mop1F1 were mapped to the B73 reference genome (v4), and the reads from Mo17 were mapped to the pseudo-Mo17 genome sequences using bowtie (Langmead et al. 2009; Jiao et al. 2017), as was done for our methylation analysis. For the parents, only perfectly and uniquely mapped reads (-v 0 -m 1) were kept, and 1 mismatch (-v 1 -m 1) was allowed for the F1 hybrids. The small RNA values were adjusted to total abundance of all mature microRNAs following the previous research to remove the artificial increase of 22-nt siRNAs in mop1 mutants caused by normalization (Nobuta et al. 2008). The intersect module in BEDTools was used to compare the mapping results (sam files) to the positions of DMRs to obtain the 24-nt small RNA reads that are in the DMRs (Quinlan and Hall 2010). These 24-nt small RNAs were used to calculate the expression of small RNAs of the DMRs. To access allele-specific small RNA expression, samtools mpileup and SNPs at small RNAs between B73 and Mo17 were used (Danecek et al. 2021).

#### Analysis of mRNA-seq data

The mRNAs from the same genetic materials were sequenced with 2 biological replicates. The raw reads were quality controlled by FastQC, and the low-quality reads and the adapter sequences were removed by Trimmomatic (Bolger et al. 2014). We mapped the cleaned reads of B73, WTF1, and mop1F1 to the B73 reference genome (v4; Jiao et al. 2017) and the reads from Mo17 to the pseudo-Mo17 genome that was generated by replacing the B73 genome with the SNPs between Mo17 and B73 using Hisat2 with 1 mismatch (Kim et al. 2019). Next, HTSeq-count was used to calculate the total number of reads of each gene (Putri et al. 2022). These values were loaded to DESeq2 to identify genes that were differentially expressed between WTF1 and parents and between WTF1 and mop1F1 (Love et al. 2014). To determine allele-specific expression of each gene in F1, the mpileup functions in samtools and SNPs between B73 and Mo17 were used to access allele-specific reads (Danecek et al. 2021), which were further used in DESeq2 to identify differential expression of the 2 alleles (Love et al. 2014).

#### Statistical analyses

Comparisons of the abundance and ratios of 24-nt siRNAs, gene length and expression values, DNA methylation and histone modification levels, and SNP density between high parent and low parent, between WTF1 and MPV, between WTF1 and mop1F1, between TCM and TCdM, and between 16 suppressed and 31 enhanced genes were conducted by Student's

t test using the SAS software. All the detailed information of each statistical test and significance is provided in the legends of the figures.

#### **Accession numbers**

The raw and processed data of whole genome bisulfite, mRNA, and small RNA sequencing presented in this study have been deposited in NCBI Gene Expression Omnibus under the accession number GSE222155.

#### **Acknowledgments**

We are grateful to Nathan M. Springer and Karen M. McGinnis for critical reading of the manuscript. We thank the Ohio Supercomputer Center for providing us with the computational resources to perform the analysis.

#### **Author contributions**

M.Z. conceived and designed the experiments. B.L. and M.Z. performed the experiment. B.L., D.Y., D.W., and M.Z. analyzed the data. B.L. and M.Z. wrote the original draft, and C.L., J.W., and D.L. reviewed and edited the manuscript.

#### Supplementary data

The following materials are available in the online version of this article.

**Supplementary Figure S1.** Whole genome levels of DNA methylation among parents, hybrids, and mutants.

**Supplementary Figure S2.** CHH methylation is globally increased in hybrids.

**Supplementary Figure S3.** The length distribution of the DMRs identified between parents.

**Supplementary Figure S4.** DMRs between the authentic Mo17 and the pseudo-B73 genome.

**Supplementary Figure S5.** Genomic distribution of unchanged parental DMRs.

**Supplementary Figure S6.** Methylation changes at the unchanged DMRs.

**Supplementary Figure S7.** Genomic distribution of *mop1*-affected DMRs.

**Supplementary Figure S8.** The production of 24-nt siRNAs from gene bodies and flanking regions.

**Supplementary Figure S9.** The high parent has significantly more 24-nt siRNAs.

**Supplementary Figure \$10.** Comparisons of 24-nt siRNAs at unchanged, TCM, and TCdM DMRs.

**Supplementary Figure S11.** Expression of genes involved in the transcriptional gene silencing pathway.

**Supplementary Figure S12.** CHH methylation is associated with both suppressed and enhanced expression of their flanking genes.

**Supplementary Figure S13.** Newly induced CG and CHG DMRs are largely located in TEs.

**Supplementary Figure S14.** Most new CG and CHG DMRs lose methylation, and most new CHH DMRs gain methylation in WTF1.

**Supplementary Figure S15.** No significant changes in small RNAs between the 2 parents and between the hybrids and parents.

**Supplementary Figure S16.** Inheritance of newly triggered methylation at CG and CHG TCM DMRs in the backcrossed generation.

**Supplementary Figure S17.** Inheritance of newly triggered methylation at CHH TCM DMRs in the backcrossed generation.

**Supplementary Table S1.** The summary of raw reads of different samples.

**Supplementary Table S2.** The overall patterns of cytosine methylation in parents, WTF1, and mutant F1.

**Supplementary Table S3.** DMRs identified between parents (B73 and Mo17).

**Supplementary Table S4.** Number of changed DMRs in the other 2 cytosine contexts at the *mop1*-affected CG, CHG, and CHH DMRs.

**Supplementary Table S5.** The expression values of 24-nt siRNAs between high parent (HP) and low parent (LP) at the parental DMRs.

**Supplementary Table S6.** Differentially expressed genes involved in the transcriptional gene silencing pathway between parents.

**Supplementary Table S7.** Differentially expressed genes involved in the transcriptional gene silencing pathway between MPV and F1.

**Supplementary Table S8.** Inheritance of CG and CHG TCM and TCdM in the backcrossed generation (BC1).

**Supplementary Table S9.** Inheritance of CHH TCM and TCdM in the backcrossed generation (BC1).

#### **Funding**

This work was supported by the National Institute of General Medical Sciences of the National Institutes of Health under Award Numbers P20GM103476 to D.W. and R15GM135874 to M.Z., and the National Science Foundation (Plant Genome Research Program) under Award Number IOS2306220 to M.Z.

Conflict of interest statement. The authors declare that they have no conflict of interests.

#### Data availability

The data underlying this article are available in the article and in its online supplementary material.

#### References

- Alleman M, Sidorenko L, McGinnis K, Seshadri V, Dorweiler JE, White J, Sikkink K, Chandler VL. An RNA-dependent RNA polymerase is required for paramutation in maize. Nature 2006:442(7100): 295–298. https://doi.org/10.1038/nature04884
- **Arteaga-Vazquez MA, Chandler VL**. Paramutation in maize: RNA mediated trans-generational gene silencing. Curr Opin Genet Dev. 2010;**20**(2):156–163. https://doi.org/10.1016/j.gde.2010.01.008

- Barber WT, Zhang W, Win H, Varala KK, Dorweiler JE, Hudson ME, Moose SP. Repeat associated small RNAs vary among parents and following hybridization in maize. Proc Natl Acad Sci U S A. 2012: 109(26):10444–10449. https://doi.org/10.1073/pnas.1202073109
- **Batista RA, Kohler C.** Genomic imprinting in plants-revisiting existing models. Genes Dev. 2020:**34**(1–2):24–36. https://doi.org/10.1101/gad.332924.119
- **Bolger AM, Lohse M, Usadel B**. Trimmomatic: a flexible trimmer for Illumina sequence data. Bioinformatics 2014:**30**(15):2114–2120. https://doi.org/10.1093/bioinformatics/btu170
- Bukowski R, Guo X, Lu Y, Zou C, He B, Rong Z, Wang B, Xu D, Yang B, Xie C, et al. Construction of the third-generation Zea mays haplotype map. Gigascience 2018:7(4):1–12. https://doi.org/10.1093/gigascience/gix134
- Cao S, Wang L, Han T, Ye W, Liu Y, Sun Y, Moose SP, Song Q, Chen ZJ. Small RNAs mediate transgenerational inheritance of genome-wide trans-acting epialleles in maize. Genome Biol. 2022:23(1):53. https://doi.org/10.1186/s13059-022-02614-0
- Chen J, Wang Z, Tan K, Huang W, Shi J, Li T, Hu J, Wang K, Wang C, Xin B, et al. A complete telomere-to-telomere assembly of the maize genome. Nat Genet. 2023:55(7):1221–1231. https://doi.org/10.1038/s41588-023-01419-6
- Chodavarapu RK, Feng S, Ding B, Simon SA, Lopez D, Jia Y, Wang GL, Meyers BC, Jacobsen SE, Pellegrini M. Transcriptome and methylome interactions in rice hybrids. Proc Natl Acad Sci U S A. 2012: 109(30):12040–12045. https://doi.org/10.1073/pnas.1209297109
- Danecek P, Bonfield JK, Liddle J, Marshall J, Ohan V, Pollard MO, Whitwham A, Keane T, McCarthy SA, Davies RM, et al. Twelve years of SAMtools and BCFtools. Gigascience 2021:10(2):giab008. https://doi.org/10.1093/gigascience/giab008
- Erdmann RM, Picard CL. RNA-directed DNA methylation. PLoS Genet. 2020:16(10):e1009034. https://doi.org/10.1371/journal.pgen.1009034
- Gent JI, Ellis NA, Guo L, Harkess AE, Yao Y, Zhang X, Dawe RK. CHH islands: de novo DNA methylation in near-gene chromatin regulation in maize. Genome Res. 2013:23(4):628–637. https://doi.org/10.1101/gr.146985.112
- Gent JI, Madzima TF, Bader R, Kent MR, Zhang X, Stam M, McGinnis KM, Dawe RK. Accessible DNA and relative depletion of H3K9me2 at maize loci undergoing RNA-directed DNA methylation. Plant Cell. 2014;26(12):4903–4917. https://doi.org/10.1105/tpc.114.130427
- Gobel U, Arce AL, He F, Rico A, Schmitz G, de Meaux J. Robustness of transposable element regulation but no genomic shock observed in interspecific *Arabidopsis* hybrids. Genome Biol Evol. 2018:**10**(6): 1403–1415. https://doi.org/10.1093/gbe/evy095
- Greaves IK, Eichten SR, Groszmann M, Wang A, Ying H, Peacock WJ, Dennis ES. Twenty-four-nucleotide siRNAs produce heritable transchromosomal methylation in F1 *Arabidopsis* hybrids. Proc Natl Acad Sci U S A. 2016:113(44):E6895–E6902. https://doi.org/10.1073/pnas. 1613623113
- Greaves IK, Gonzalez-Bayon R, Wang L, Zhu A, Liu PC, Groszmann M, Peacock WJ, Dennis ES. Epigenetic changes in hybrids. Plant Physiol. 2015:168(4):1197–1205. https://doi.org/10.1104/pp.15.00231
- Greaves IK, Groszmann M, Wang A, Peacock WJ, Dennis ES. Inheritance of trans chromosomal methylation patterns from *Arabidopsis* F1 HYBRIDS. Proc Natl Acad Sci U S A. 2014:**111**(5): 2017–2022. https://doi.org/10.1073/pnas.1323656111
- **Greaves IK, Groszmann M, Ying H, Taylor JM, Peacock WJ, Dennis ES.** Trans chromosomal methylation in *Arabidopsis* hybrids. Proc Natl Acad Sci U S A. 2012:**109**(9):3570–3575. https://doi.org/10. 1073/pnas.1201043109
- Groszmann M, Greaves IK, Albertyn ZI, Scofield GN, Peacock WJ, Dennis ES. Changes in 24-nt siRNA levels in *Arabidopsis* hybrids suggest an epigenetic contribution to hybrid vigor. Proc Natl Acad Sci U S A. 2011:108(6):2617–2622. https://doi.org/10.1073/pnas.1019217108
- **Guo W, Wang D, Lisch D**. RNA-directed DNA methylation prevents rapid and heritable reversal of transposon silencing under heat stress in

- Zea mays. PLoS Genet. 2021:17(6):e1009326. https://doi.org/10.1371/ journal.pgen.1009326
- He G, Chen B, Wang X, Li X, Li J, He H, Yang M, Lu L, Qi Y, Wang X, et al. Conservation and divergence of transcriptomic and epigenomic variation in maize hybrids. Genome Biol. 2013:14(6):R57. https://doi.org/10.1186/gb-2013-14-6-r57
- He G, Zhu X, Elling AA, Chen L, Wang X, Guo L, Liang M, He H, Zhang H, Chen F, et al. Global epigenetic and transcriptional trends among two rice subspecies and their reciprocal hybrids. Plant Cell. 2010: 22(1):17-33. https://doi.org/10.1105/tpc.109.072041
- He XJ, Chen T, Zhu JK. Regulation and function of DNA methylation in plants and animals. Cell Res. 2011:21(3):442-465. https://doi.org/10. 1038/cr.2011.23
- Hollick JB. Paramutation and related phenomena in diverse species. Nat Rev Genet. 2017:18(1):5-23. https://doi.org/10.1038/nrg.2016.
- Hollister JD, Gaut BS. Epigenetic silencing of transposable elements: a trade-off between reduced transposition and deleterious effects on neighboring gene expression. Genome Res. 2009:19(8):1419-1428. https://doi.org/10.1101/gr.091678.109
- Hufford MB, Seetharam AS, Woodhouse MR, Chougule KM, Ou S, Liu J, Ricci WA, Guo T, Olson A, Qiu Y, et al. De novo assembly, annotation, and comparative analysis of 26 diverse maize genomes. Science 2021:373(6555):655-662. https://doi.org/10.1126/science.
- Ishikawa R, Kinoshita T. Epigenetic programming: the challenge to species hybridization. Mol Plant. 2009:2(4):589-599. https://doi.org/ 10.1093/mp/ssp028
- Jiao Y, Peluso P, Shi J, Liang T, Stitzer MC, Wang B, Campbell MS, Stein JC, Wei X, Chin CS, et al. Improved maize reference genome with single-molecule technologies. Nature 2017:546(7659):524-527. https://doi.org/10.1038/nature22971
- Josefsson C, Dilkes B, Comai L. Parent-dependent loss of gene silencing during interspecies hybridization. Curr Biol. 2006:16(13): 1322-1328. https://doi.org/10.1016/j.cub.2006.05.045
- Juhling F, Kretzmer H, Bernhart SH, Otto C, Stadler PF, Hoffmann S. Metilene: fast and sensitive calling of differentially methylated regions from bisulfite sequencing data. Genome Res. 2016:26(2): 256-262. https://doi.org/10.1101/gr.196394.115
- Junaid A, Kumar H, Rao AR, Patil AN, Singh NK, Gaikwad K. Unravelling the epigenomic interactions between parental inbreds resulting in an altered hybrid methylome in pigeonpea. DNA Res. 2018:25(4):361-373. https://doi.org/10.1093/dnares/dsy008
- Kakoulidou I, Johannes F. DNA methylation remodeling in F1 hybrids. Plant J. 2023. https://doi.org/10.1111/tpj.16137
- Kenan-Eichler M, Leshkowitz D, Tal L, Noor E, Melamed-Bessudo C, Feldman M, Levy AA. Wheat hybridization and polyploidization results in deregulation of small RNAs. Genetics 2011:188(2):263-272. https://doi.org/10.1534/genetics.111.128348
- Kim D, Paggi JM, Park C, Bennett C, Salzberg SL. Graph-based genome alignment and genotyping with HISAT2 and HISAT-genotype. Nat Biotechnol. 2019:37(8):907-915. https://doi.org/10.1038/s41587-019-0201-4
- Krueger F, Andrews SR. Bismark: a flexible aligner and methylation caller for Bisulfite-Seq applications. Bioinformatics 2011:27(11): 1571-1572. https://doi.org/10.1093/bioinformatics/btr167
- Langmead B, Trapnell C, Pop M, Salzberg SL. Ultrafast and memory-efficient alignment of short DNA sequences to the human genome. Genome Biol. 2009:10(3):R25. https://doi.org/10.1186/gb-2009-10-3-r25
- Law JA, Jacobsen SE. Establishing, maintaining and modifying DNA methylation patterns in plants and animals. Nat Rev Genet. 2010:**11**(3):204–220. https://doi.org/10.1038/nrg2719
- Lewsey MG, Hardcastle TJ, Melnyk CW, Molnar A, Valli A, UrichMA, Nery JR, Baulcombe DC, Ecker JR. Mobile small RNAs regulate genome-wide DNA methylation. Proc Natl Acad Sci U S A. 2016: 113(6):E801-E810. https://doi.org/10.1073/pnas.1515072113

- Li H, Durbin R. Fast and accurate short read alignment with Burrows-Wheeler transform. Bioinformatics 2009:25(14):1754-1760. https:// doi.org/10.1093/bioinformatics/btp324
- Li Q, Eichten SR, Hermanson PJ, Springer NM. Inheritance patterns and stability of DNA methylation variation in maize near-isogenic lines. Genetics 2014a:**196**(3):667–676. https://doi.org/10.1534/ genetics.113.158980
- Li Q, Eichten SR, Hermanson PJ, Zaunbrecher VM, Song J, Wendt J, Rosenbaum H, Madzima TF, Sloan AE, Huang J, et al. Genetic perturbation of the maize methylome. Plant Cell. 2014b:26(12): 4602-4616. https://doi.org/10.1105/tpc.114.133140
- Li Q, Gent JI, Zynda G, Song J, Makarevitch I, Hirsch CD, Hirsch CN, Dawe RK, Madzima TF, McGinnis KM, et al. RNA-directed DNA methylation enforces boundaries between heterochromatin and euchromatin in the maize genome. Proc Natl Acad Sci U S A. 2015a:
  - **112**(47):14728–14733. https://doi.org/10.1073/pnas.1514680112
- Li Q, Song J, West PT, Zynda G, Eichten SR, Vaughn MW, Springer NM. Examining the causes and consequences of context-specific differential DNA methylation in maize. Plant Physiol. 2015b:168(4): 1262-1274. https://doi.org/10.1104/pp.15.00052
- Li T, Yin L, Stoll CE, Lisch D, Zhao M. Conserved noncoding sequences and de novo mutator insertion alleles are imprinted in maize. Plant Physiol. 2023:**191**(1):299–316. https://doi.org/10.1093/plphys/kiac459
- Liu B, Iwata-Otsubo A, Yang D, Baker RL, Liang C, Jackson SA, Liu S, Ma J, Zhao M. Analysis of CACTA transposase genes unveils the mechanism of intron loss and distinct small RNA silencing pathways underlying divergent evolution of Brassica genomes. Plant J. 2021:105(1):34-48. https://doi.org/10.1111/tpj.15037
- Liu B, Zhao M. How transposable elements are recognized and epigenetically silenced in plants? Curr Opin Plant Biol. 2023:75:102428. https://doi.org/10.1016/j.pbi.2023.102428
- Love MI, Huber W, Anders S. Moderated estimation of fold change and dispersion for RNA-Seq data with DESeq2. Genome Biol. 2014: 15(12):550. https://doi.org/10.1186/s13059-014-0550-8
- Ma X, Xing F, Jia Q, Zhang Q, Hu T, Wu B, Shao L, Zhao Y, Zhang Q, **Zhou DX**. Parental variation in CHG methylation is associated with allelic-specific expression in elite hybrid rice. Plant Physiol. 2021: 186(2):1025-1041. https://doi.org/10.1093/plphys/kiab088
- Martin GT, Seymour DK, Gaut BS. CHH methylation islands: a nonconserved feature of grass genomes that is positively associated with transposable elements but negatively associated with genebody methylation. Genome Biol Evol. 2021:13(8):evab144. https:// doi.org/10.1093/gbe/evab144
- Matzke MA, Kanno T, Matzke AJ. RNA-directed DNA methylation: the evolution of a complex epigenetic pathway in flowering plants. Annu Rev Plant Biol. 2015:66(1):243-267. https://doi.org/10.1146/ annurev-arplant-043014-114633
- Matzke MA, Mosher RA. RNA-directed DNA methylation: an epigenetic pathway of increasing complexity. Nat Rev Genet. 2014:15(6): 394-408. https://doi.org/10.1038/nrg3683
- McClintock B. The significance of responses of the genome to challenge. Science. 1984:226(4676):792-801. https://doi.org/10. 1126/science.15739260
- Nobuta K, Lu C, Shrivastava R, Pillay M, De Paoli E, Accerbi M, Arteaga-Vazquez M, Sidorenko L, Jeong DH, Yen Y, et al. Distinct size distribution of endogeneous siRNAs in maize: evidence from deep sequencing in the mop1-1 mutant. Proc Natl Acad Sci U S A. 2008:**105**(39):14958–14963. https://doi.org/10.1073/pnas.0808066105
- Putri GH, Anders S, Pyl PT, Pimanda JE, Zanini F. Analysing highthroughput sequencing data in Python with HTSeq 2.0. Bioinformatics 2022:38(10):2943-2945. https://doi.org/10.1093/ bioinformatics/btac166
- Qin J, Mo R, Li H, Ni Z, Sun Q, Liu Z. The transcriptional and splicing changes caused by hybridization can be globally recovered by genome doubling during allopolyploidization. Mol Biol Evol. 2021: 38(6):2513-2519. https://doi.org/10.1093/molbev/msab045

- **Quinlan AR, Hall IM**. BEDTools: a flexible suite of utilities for comparing genomic features. Bioinformatics 2010:**26**(6):841–842. https://doi.org/10.1093/bioinformatics/btq033
- Regulski M, Lu Z, Kendall J, Donoghue MT, Reinders J, Llaca V, Deschamps S, Smith A, Levy D, McCombie WR, et al. The maize methylome influences mRNA splice sites and reveals widespread paramutation-like switches guided by small RNA. Genome Res. 2013: 23(10):1651–1662. https://doi.org/10.1101/gr.153510.112
- Ricci WA, Lu Z, Ji L, Marand AP, Ethridge CL, Murphy NG, Noshay JM, Galli M, Mejia-Guerra MK, Colome-Tatche M, et al. Widespread long-range cis-regulatory elements in the maize genome. Nat Plants. 2019:5(12):1237–1249. https://doi.org/10.1038/s41477-019-0547-0
- **Rodrigues JA, Zilberman D.** Evolution and function of genomic imprinting in plants. Genes Dev. 2015:**29**(24):2517–2531. https://doi.org/10.1101/gad.269902.115
- Schmitz RJ, He Y, Valdes-Lopez O, Khan SM, Joshi T, Urich MA, Nery JR, Diers B, Xu D, Stacey G, et al. Epigenome-wide inheritance of cytosine methylation variants in a recombinant inbred population. Genome Res. 2013:23(10):1663–1674. https://doi.org/10.1101/gr. 152538.112
- Schmitz RJ, Schultz MD, Lewsey MG, O'Malley RC, Urich MA, Libiger O, Schork NJ, Ecker JR. Transgenerational epigenetic instability is a source of novel methylation variants. Science 2011:334(6054): 369–373. https://doi.org/10.1126/science.1212959
- Schultz MD, Schmitz RJ, Ecker JR. 'Leveling' the playing field for analyses of single-base resolution DNA methylomes. Trends Genet. 2012;28(12):583–585. https://doi.org/10.1016/j.tig.2012.10.012
- Shen H, He H, Li J, Chen W, Wang X, Guo L, Peng Z, He G, Zhong S, Qi Y, et al. Genome-wide analysis of DNA methylation and gene expression changes in two *Arabidopsis* ecotypes and their reciprocal hybrids. Plant Cell. 2012:**24**(3):875–892. https://doi.org/10.1105/tpc. 111.094870
- Shivaprasad PV, Dunn RM, Santos BA, Bassett A, Baulcombe DC. Extraordinary transgressive phenotypes of hybrid tomato are influenced by epigenetics and small silencing RNAs. EMBO J. 2012:31(2):257–266. https://doi.org/10.1038/emboj.2011.458

- Stroud H, Do T, Du J, Zhong X, Feng S, Johnson L, Patel DJ, Jacobsen SE. Non-CG methylation patterns shape the epigenetic landscape in *Arabidopsis*. Nat Struct Mol Biol. 2014:21(1):64–72. https://doi.org/10.1038/nsmb.2735
- To TK, Nishizawa Y, Inagaki S, Tarutani Y, Tominaga S, Toyoda A, Fujiyama A, Berger F, Kakutani T. RNA interference-independent reprogramming of DNA methylation in *Arabidopsis*. Nat Plants. 2020:6(12):1455–1467. https://doi.org/10.1038/s41477-020-00810-z
- Woodhouse MR, Freeling M, Lisch D. The mop1 (mediator of paramutation1) mutant progressively reactivates one of the two genes encoded by the MuDR transposon in maize. Genetics 2006:172(1): 579–592. https://doi.org/10.1534/genetics.105.051383
- Xu G, Lyu J, Li Q, Liu H, Wang D, Zhang M, Springer NM, Ross-Ibarra J, Yang J. Evolutionary and functional genomics of DNA methylation in maize domestication and improvement. Nat Commun. 2020:11(1):5539. https://doi.org/10.1038/s41467-020-19333-4
- Yin L, Xu G, Yang J, Zhao M. The heterogeneity in the landscape of gene dominance in maize is accompanied by unique chromatin environments. Mol Biol Evol. 2022:39(10):msac198. https://doi.org/10.1093/molbev/msac198
- Zhang Q, Wang D, Lang Z, He L, Yang L, Zeng L, Li Y, Zhao C, Huang H, Zhang H, et al. Methylation interactions in *Arabidopsis* hybrids require RNA-directed DNA methylation and are influenced by genetic variation. Proc Natl Acad Sci U S A. 2016:113:E4248–E4256. https://doi.org/10.1073/pnas.1607851113
- Zhao M, Ku JC, Liu B, Yang D, Yin L, Ferrell TJ, Stoll CE, Guo W, Zhang X, Wang D, et al. The mop1 mutation affects the recombination landscape in maize. Proc Natl Acad Sci U S A. 2021:118(7): e2009475118. https://doi.org/10.1073/pnas.2009475118
- Zhao M, Zhang B, Lisch D, Ma J. Patterns and consequences of subgenome differentiation provide insights into the nature of paleopolyploidy in plants. Plant Cell. 2017:29(12):2974–2994. https://doi.org/10.1105/tpc.17.00595
- Zilberman D, Gehring M, Tran RK, Ballinger T, Henikoff S. Genomewide analysis of *Arabidopsis thaliana* DNA methylation uncovers an interdependence between methylation and transcription. Nat Genet. 2007;39(1):61–69. https://doi.org/10.1038/ng1929